DOI:10.14753/SE.2012.1675

Studies on Cyclophilin-D and NAADP on Ca^{2+}-mediated events

PhD thesis

Miklós Mándi, MD

Semmelweis University
Neurosciences ('János Szentágothai') PhD School
Functional Neurosciences Program

Supervisors: Veronika Ádám, MD, DSc

Official reviewers: Balázs Sümegi, MD, DSc
Gábor Bánhegyi, MD, DSc

Chairman of committee: Erzsébet Ligeti, MD, DSc

Members of committee: Zsolt Liposits, MD, DSc
Csaba Sőti, MD, PhD

Budapest, 2011

Table of contents

Abbreviations

$\Delta\Psi_m$:	membrane potential
2-BO:	2-bromooctanoate
ACh:	acethylcholine
ADP:	adenosine diphosphate
ADPRCs:	ADP-ribosyl cyclase enzyme family
AIF:	apoptosis-inducing factor
ANT:	adenine nucleotide translocase
AP_5A:	P_1,P_5-di-(adenosine-5′)-pentaphosphate
AT-II:	angiotensin II
ATP:	adenosine triphosphate
ATR:	atraciloside
BCECF:	2’,7’-bis(carboxyethyl)-5,6-carboxyfluorescein
BKA:	bongkrekic acid
BSA:	bovine serum albumin
cADPR(P):	cyclic adenosine dinucleotide-ribose (phosphate)
CaGreen:	Calcium Green 5N
cATR:	carboxyatractyloside
CCK:	cholecystokinine
CICR:	Ca^{2+}-induced Ca^{2+} release
CK:	creatine kinase
CL:	cardiolipin
CypD:	cyclophilin-D
Cyt c:	cytochrome c
CysA:	cyclosporine-A
DAG:	diacyl-glycerol
DMSO:	dimethyl-sulfoxide
DTT:	dithiothreitole
EC_{50}:	50%-excitation concentration
ER:	endoplasmic reticulum
ETC:	electron transport chain

EDTA: ethylenediamine-tetraacetic acid

EGTA: ethylene glycol-bis(2-aminoethylether)-N,N,N′,N′-tetraacetic acid

E_{rev}_ANT: reversal potential of the ANT

E_{rev}_ATPase: reversal potential of the F_0F_1ATPase

FCCP: carbonyl cyanide 4-(trifluoromethoxy)-phenylhydrazone

FFA: free fatty acid

GPN: glycyl-phenylalanyl-naphtylamide

Hepes: 4-(2-hydroxyethyl)-1-piperazineethanesulfonic acid

HK: hexokinase

IC_{50}: 50%-inhibition concentration

IMM: inner mitochondrial membrane

$InsP_3$: D-*myo*-inositol-1,4,5-trisphosphate

mBR: peripheral mitochondrial benzodiazepine receptor

MCF: mitochondrial carrier family

MgG: magnesium green

MOPS: 3-(N-morpholino)-propanesulfonic acid

$NAD(P)^+$: nicotinamide-adenine dinucleotide (phosphate)

NAADP: nicotinic acid-adenine dinucleotide phosphate

NCE: Na^+-Ca^{2+} exchanger

NICE: Na^+-independent Ca^{2+} exchanger (H^+-Ca^{2+} exchanger)

OMM: outer mitochondrial membrane

pH_{in}: mitochondrial matrix pH

pH_o: extramitochondrial pH

P_i: inorganic phosphate

PP_i: inorganic pyrophaosphate

PiC: phosphate carrier

PLA_2: phospholipase A_2

pmf: protonmotive force

PMSF: phenylmethylsulfonyl fluoride

PN: pyridine nucleotides

PPIase: peptidyl-prolyl *cis-trans* isomerase

(m)PTP: (mitochondrial) permeability transition pore

RaM: rapid (Ca^{2+}) uptake mode

ROS: reactive oxygen species

RuRed: ruthenium-red

RyR: ryanodine receptor

SCN^-: thiocyanate

SERCA: sarco(endo)plasmic reticulum Ca^{2+}-ATPase

SF 6847 (Tyrphostin 9, RG-50872, Malonaben): 2-[[3,5-bis(1,1-dimethylethyl)-4-hydroxyphenyl]methylene]-propanedinitrile

Sf-A: Sanglifehrin-A

SR: sarcoplasmic reticulum

TMPD: N,N,N′,N′-tetramethyl-p-phenylenediamine

TPCN2: two-pore cation channel, type 2

Tris: tris-(hydroxymethyl)-aminomethane

TRP: transient receptor potential channel

VDAC: voltage-dependent anion channel

WT: wild type

1. Introduction

Calcium is one of the most versatile and important intracellular messengers in living cells and organisms. Ca^{2+} signalling is involved in the control of numerous biological processes [1;2]. For example, Ca^{2+} is essential for oocyte fertilization, synaptic plasticity, muscle cell contraction, gene expression, enzyme / neurotransmitter secretion and cell proliferation, as well as cell death (both apoptosis and necrosis). Ca^{2+} signals are intracellular relays of triggering events, such as depolarization, hormone or neurotransmitter stimulations, in order to control cell functions [1;2]. Ca^{2+} signals are not all-or-none events; they vary greatly in amplitude, duration and localization. Cytosolic Ca^{2+} signals can be generated by activation of Ca^{2+} entry and/or by mobilization of Ca^{2+} from intracellular stores. At the level of plasma membrane, Ca^{2+} influx occurs through several types of channels, such as voltage-gated channels, ligand-gated channels and transient receptor potential (TRP) ion channels [3-5]. Ca^{2+} is also stored in most organelles, including endoplasmic reticulum (ER), mitochondria, lysosomes, secretory granules, Golgi apparatus and nuclear envelope [6;7]. Thus, compartmentalization of Ca^{2+} to the extracellular matrix or to intracellular organelles is a crucial element of Ca^{2+} signalling [8]. Moreover, Ca^{2+} release from some of these stores can be triggered by intracellular second messengers. Ca^{2+} fluxes display complex spatial and temporal signatures, enabling more information to be encoded by Ca^{2+} signals. To meet the demands of this complexity, cells rely on precise regulation of Ca^{2+} channel activity [1].

The present thesis focuses on the role of cyclophilin-D in Ca^{2+}-triggered mitochondrial permeability transition and Ca^{2+} release from the cytosolic acidic Ca^{2+} stores.

1.1. Mitochondria as Ca^{2+} stores

The importance of mitochondria in cellular Ca^{2+} homeostasis was questioned for a long period of time when the ER was identified as the main inositol-1,4,5-trisphosphate ($InsP_3$)-dependent intracellular Ca^{2+} store [9;10]. Subsequently, the general consensus was that mitochondria would form a 'Ca^{2+} sink' [2;11;12], since it was hypothesized that the well-known low affinity but high capacity mitochondrial Ca^{2+} uptake mechanisms would only be significant under conditions of high-amplitude or prolonged $[Ca^{2+}]_c$ increases, i.e. in the Ca^{2+} overload. However, changes of $[Ca^{2+}]_c$ in response to physiologically relevant stimuli were shown to coexist with rapid modulations of the $[Ca^{2+}]_m$ [13;14], proving that mitochondria indeed play a more complex role in Ca^{2+} signalling [15]. Moreover, three mitochondrial enzymes participating in key steps of the intermediate metabolism (the pyruvate-, α-ketoglutarate- and isocitrate-dehydrogenases) are also regulated by Ca^{2+}, a notion that would imply that $[Ca^{2+}]_m$ should be suited to follow the physiological $[Ca^{2+}]_c$ events of the cell [16;17]. Uptake and efflux of Ca^{2+} in mitochondria occur by different processes (see **Figure 1**).

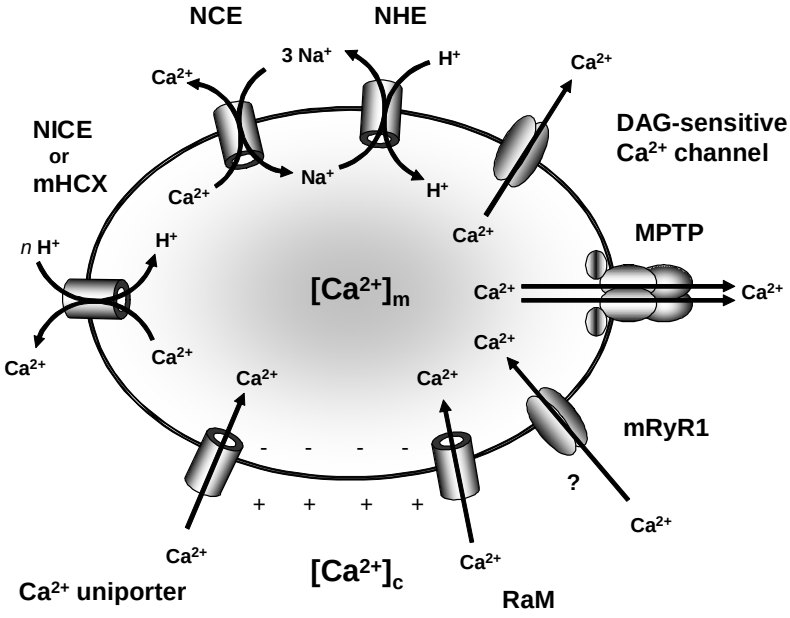

Figure 1. Pathways for Ca^{2+} uptake and release in mitochondria.

1.1.1. Mechanisms for Ca^{2+} uptake into mitochondria

Generally, the mitochondrial inner membrane potential ($\Delta\Psi_m$, that is usually between -150 and -180 mV) is the driving force of the two major mechanisms of Ca^{2+} entry to the mitochondria identified to date: the Ca^{2+} uniporter and the rapid uptake mode (RaM) [18]. The Ca^{2+} uniporter 'in vitro' is a low-affinity and high capacity transporter that is non-competitively blocked by ruthenium compounds (e.g. Ruthenium Red [RuRed] [19;20], Ru360 [21]) or inhibited in a mainly competitive manner by divalent cations - that are themselves transported by the uniporter (e.g. Sr^{2+}, Mn^{2+}, Ba^{2+} and lanthanides), and activated by ATP, physiological concentrations of spermine and taurine [12;21-23]. In permeabilized cells however, the half-maximal activation ($K_{0.5}$) for mitochondrial Ca^{2+} transport rate, presumably through the uniporter, was found to be 3-fold higher than 'in vitro' [24;25]. Hence it is possible that the affinity of the uniporter is higher in a cellular environment (possibly due to the presence of spermine or taurine or other intracellular factors). Moreover, regarding the factors that modulate Ca^{2+} influx through the uniporter, the most important is the extramitochondrial [Ca^{2+}]. Likewise, the rate of Ca^{2+} uptake through the uniporter shows a biphasic dependence on cytosolic Ca^{2+} in the presence of functional calmodulin [26;27] and physiological [Mg^{2+}] [28]. Thus, the uniporter may function indeed at physiological pCa. On the other hand, evidence has been presented for the formation of high Ca^{2+} microdomains [29-31], especially in the ER-mitochondrial junctions, in which the local Ca^{2+}-load can be enough to activate the Ca^{2+} uniporter even if its affinity for Ca^{2+} is as low as 'in vitro' [29-31].

In contrast, the other major pathway for mitochondrial Ca^{2+} uptake, RaM is a high affinity and high initial conductance Ca^{2+} transporter responding to small, but rapid Ca^{2+} transients of the cytoplasm [18;32]. RaM is inhibited by RuRed as well as Ca^{2+} itself, which exerts rapid inactivation of RaM following its activation [33].

Thus, RaM takes sufficient amounts of Ca^{2+} for the activation of the Ca^{2+}-sensitive dehydrogenases into the matrix [18] without causing Ca^{2+} overloading of mitochondria [34]. The molecular identity of both the Ca^{2+} uniporter and RaM has not yet been clarified and it is still uncertain whether RaM could be defined as a different 'mode of transport' through the uniporter or it may be a molecularly distinct entity [35].

On the other hand, a mitochondrial ryanodine receptor (mRyR1) has been identified in the inner membrane of rat heart mitochondria solely by Beutner et al. that shared pharmaco-kinetic properties with the skeletal type RyR (RyR1) [36-38]. It has been suggested that mRyR1 may play an important role in the excitation-metabolism coupling in rat heart mitochondria, thus behaving as a Ca^{2+} uptake mechanism [37;38].

1.1.2. Ca^{2+} efflux pathways from mitochondria

In the mitochondria of vertebrates, two different routes for Ca^{2+} efflux have been characterized: one is Na^+-dependent (Na^+/Ca^{2+} exchanger, mNCX or NCE) that is coupled to Na^+/H^+ exchange, while the other is Na^+-independent (H^+/Ca^{2+} exchanger, mHCX or NICE) [39]. The stoichiometry of NCE is $3Na^+:1Ca^{2+}$ [23;34;39], while NICE shows a stiochiometry of $nH^+:1Ca^{2+}$, where n is probably >2 [39], thus both are electrogenic. There are many established blockers of NCE including tetraphenyl phosphonium, trifluroperazine, diltiazem, verapamil, clonazepam, amiloride, and CGP-37157, while there are only few known inhibitors of NICE such as tetraphenyl phosphonium, cyanide and low levels of uncouplers [34]. The dominant Ca^{2+} efflux mechanism in heart, brain, skeletal muscle, parotid gland, adrenal cortex, brown fat and endothelial mitochondria is NCE [25;34;40], while NICE is mainly expressed on mitochondria in non-excitable tissues e.g. liver, lung, kidney and smooth muscle [23].

A diacylglycerol (DAG)-activated cation channel has also been described as the first second-messenger induced Ca^{2+} release mechanism

in the inner membrane of different mammalian mitochondria [41]. DAG analogs have been shown to release Ca^{2+} from loaded mitochondria in a biphasic manner. A rapid and transient initial Ca^{2+} release is observed, that is not accompanied by mitochondrial swelling and likewise, it is insensitive to permeability transition inhibitors. Following a relatively slow reuptake of Ca^{2+} into mitochondria, a secondary, progressive release of Ca^{2+} occurred, that was associated with swelling and attenuated by permeability transition inhibitors [41]. The initial peak of DAGs-induced Ca^{2+} efflux is abolished by La^{3+} (1mM) and potentiated by protein kinase C inhibitors. The putative DAG sensitive channel shows receptoric properties, since the 1,2-sn-DAG analogs induce mitochondrial Ca^{2+} efflux exclusively, while other DAG analogs or substitutes, such as phorbol esters, 1,3-diacylglycerols and 1- or 2-monoacylglycerols are inactive [41]. Moreover, the forementioned channel has been demonstrated to reside in the IMM since Ca^{2+}-loaded mitoplasts devoid of outer mitochondrial membrane also exhibit DAGs-induced Ca^{2+} release. Patch clamping of brain mitoplasts revealed that DAGs induced a slightly cation-selective channel activity which is insensitive to bongkrekic acid and abolished by La^{3+} [41].

Finally, the multiprotein complex of the permeability transition pore (PTP) could represent an alternative Ca^{2+} efflux pathway from mitochondria. PTP is believed to have both a small and a large conductance state [23]. Opening of the large-conductance PTP, induced by Ca^{2+} overloading of mitochondria or by other pathophysiological conditions, leads to the collapse of the inner membrane potential ($\Delta\Psi_m$) and the release of proapoptotic factors (e.g. cytochrome c, Smac/DIABLO and apoptosis-inducting factor, AIF) [42;43] and substantial amount of Ca^{2+} is also liberated. On the other hand, the small-conductance PTP might participate in physiological Ca^{2+} handling in the form of Ca^{2+}-induced Ca^{2+} release [44].

1.1.3. Ca^{2+} storage in the mitochondrial matrix

Mithochondria are capable of accumulating vast quantities of Ca^{2+} (up to 1M) while keeping the free Ca^{2+} concentration of the matrix in the low micromolar range (~1-5 µM) [45]. This can be achieved by the formation of calcium- and phosphorus-rich precipitates in the matrix [46;47]. The relationship between the PO_4^{3-} concentration and pH shows a dependency on the third-power and the matrix pH is elevated due to pumping of H^+ by the electron transfer chain during oxidative phosphorylation [48], enabling mitochondria to maintain the low free Ca^{2+} concentration in the matrix as several folds more Ca^{2+} is stored. The precise composition of the precipitates remains uncertain, however recent studies indicate that they are composed mainly of tribasic calcium phosphate [$Ca_3(PO_4)_2$] and/or dibasic calcium phosphate ($CaHPO_4$) [47;49;50], as originally proposed nearly 40 years ago [46]. The maximal Ca^{2+} loading capacity of mitochondria is limited usually by the opening of the PTP and the Ca/P ratio of the precipitates may vary between ~1 (mainly $CaHPO_4$) and ~1.5 (mainly [$Ca_3(PO_4)_2$]) according to the Ca^{2+} load of mitochondria [50]. The acidic pH shift in the matrix upon the opening of the PTP and the dissipation of the mitochondrial membrane potential has been generally considered to play a crucial role in the mobilization of Ca^{2+} from the precipitates.

The author of the present thesis has contributed to the re-evaluation of the role of matrix acidification in uncoupler-induced Ca^{2+} release from mitochondria [51]. Our workgroup's interest was raised by the fact that in the presence of abundant P_i, small ΔpH is observed across the inner mitochondrial membrane [52]. We also relied on the fact that the ΔpH remains relatively constant within a range of extramitochondrial pH (pH_o) values [53]. We reasoned that, if matrix acidification does indeed underly the dissociation of the Ca^{2+}–phosphate complex and Ca^{2+} release by uncouplers, then at acidic pH (pH_o 6.8), complete depolarization by combined inhibition of the respiratory chain and of the

reversal of the F_0/F_1-ATPase would produce the same effect. By the same token, at alkaline pH (pH_o 7.8), complete depolarization by uncoupling would hinder the dissociation of this complex, and impair the release of sequestered Ca^{2+}. Furthermore, at alkaline pH (pH_o 7.8), complete depolarization by combined inhibition of the respiratory chain and of the reversal of the F_0F_1-ATPase should not induce release of sequestered Ca^{2+}. The experimental findings presented by our workgroup (Vajda et al., [51]) do not support the above expectations, implying that matrix acidification by uncouplers cannot be the only explanation for the release of sequestered Ca^{2+}.

1.2. Mitochondrial permeability transition pore (PTP)

1.2.1. Functions and consequences of the permeability transition

In normal aerobic conditions, the IMM always remains highly impermeable to water, ions and metabolites in order to maintain the *pmf* that is driving the ATP synthesis via the F_0-F_1 ATPase; only selective and controlled permeability via specific carriers and channels is preserved. The *pmf* is a large electrochemical driving force for protons (~200-220mV) across the IMM comprising of both $\Delta\Psi_m$ (~150-180 mV) and H^+ gradient (ΔpH), generated by the functional respiratory chain complexes pumping H^+ into the intermembrane space [54]. However, in response to ischaemic, oxidative or any other type of stress, the permeability of the IMM may increase dramatically with the formation of a voltage-dependent, non-specific pore known as the mitochondrial permeability transition pore (PTP). In it's open state, the PTP complex possesses a channel that is ~3nm vide in diameter, thus allowing the diffusion of all molecules with a molecular mass of less than 1500 Da [55;56]. As a consequence of the opening of the PTP megachannel, the $\Delta\Psi_m$ collapses and mitochondria start consuming ATP imported from the cytosol because of the reversal of the ANT and the F_0-F_1 ATPase. Moreover, the high protein concentration of the matrix exert a high colloid osmotic pressure whilst non-protein solutes equilibrate with the cystosol, bringing vast quantities of water into the matrix, thus causing matrix swelling (expansion), de-folding of the cristae of the IMM and the rupture of the OMM. With the breaking of the OMM, pro-apoptotic proteins from the intermembrane space (including cytochrome-c, Smac/DIABLO and apoptosis-inducing factor [AIF]) are released [42;43]. While the prolonged permeability transition (PT) is an all-or-none event for an individual mitochondrion, transient PTP openings can be recorded electrophysiologically in the form of conductance

'flickerings' that do not lead to swelling and are unrelated to death signals. These physiological PT-transients (also known as small conductance PTP) might encompass matrix volume and pH regulation, redox equilibrium, protein import [57], bidirectional pyridine nucleotide funnelling [58] and a fast Ca^{2+} release mechanism (see also **Section 1.1.2.**). The small conductance PTP is most probably regulated by $[Ca^{2+}]_m$, leading to a dynamic steady-state distribution of mitochondrial population with closed and open pores [57;59;60].

1.2.2. Structure of the PTP

The exact molecular composition of the PTP still remains uncertain and controversial, although numerous candidates have been investigated. Originally, based on biochemical and pharmacological studies, the PTP was proposed to consist of three major components: pore-forming voltage-dependent anionic channel (VDAC or porin) and ANT (ANT1) in the OMM and IMM respectively, moreover the regulatory cyclophilin-D (CypD) on the matrix side of the IMM [61;62].

The primary structure of monomeric ANT, including altogether 6 transmembrane domains joined by hydrophilic regions grouped in 3 repeat domains [63], is well-suited for pore-forming. The native structure of the ANT homodimer, functioning as adenine nucleotide carrier with a stoichiometry of 1:1 [64;65], is stabilized by 6 tightly bound and non-detachable cardilopin (CL) molecules per dimer at the matrix side [66]. Since the determination of the ATP-ADP steady-state exchange rate mediated by ANT plays a central role in the understanding of how mitochondria can continually provide fresh ATP to the cytosol in different conditions, our workgroup has perfected and published a new method that is an on-line, high acquisition rate and quantitative measurement of changes in Magnesium Green (MgG) fluorescence based on the different affinity of ADP^{3-} and ATP^{4-} for Mg^{2+} [53].

However, mitochondrial permeability transition still occurred in ANT1/2 double knock-out experiments [67] and VDAC1,2,3 triple knock-out experiments [68] suggesting that ANT and VDAC are not essential or replaceable in forming the PTP. A new candidate, notably an other member of the MCF/SLC25 family: the mitochondrial phosphate carrier (PiC) has been considered to be part of the PTP [61] and in the revised model, VDAC does not appear as a compulsory element (although in this case cytochrome-c release from the intermembrane space is not sufficiently elucidated).

In addition, hexokinase (HK), creatine kinase (CK), members of the Bcl-2 family and the mitochondrial benzodiazepine receptor (mBR) have also been suggested to play additional regulatory role [56;69].

1.2.3. Modulation of mitochondrial PT

Various matrix and membrane factors modulate the PTP and it's sensitivity to $[Ca^{2+}]_m$, the increase of which is the most important promoter of pore-opening (see **Table 1**). In the case of Ca^{2+} overload of mitochondria, Ca^{2+} occupies critical amino acid residues of the ANT interacting with the surrounding bound cardilopin (CL) molecules and facilitating the conformational change of ANT from

PTP inducers		PTP inhibitors
$[Ca^{2+}]_m$↑		
Ca^{2+} overload	↔	Divalent cations
		Mg^{2+}, Mn^{2+}, Sr^{2+}
		Matrix acidification, pH<7.0
'c' conformation of ANT		*'m' confromation of ANT*
Atractoligenins (ATR, cATR)	↔	Bongcrekik acid (BKA)
Cyclophilin-D PPIase activity	↔	Cyclosporin-A (CysA)
		Sangliferin-A (SfA)
		Debio 025
		Resting $\Delta\Psi_m$ (~ -180mV)
NAD$^+$ ↑	↔	*NADH* ↑
oxaloacetate		pyruvate
malonate		α-ketoglutarate
		glutamate
[ATP]↓, [ADP]↓		
P_i↑, PP_i↑		
vanadate, arsenate		
ROS, peroxide, oxidative stress		
Free fatty acids (FFA)	↔	Sphingosin, spermine, triflouperasine

Table 1. Factors inducing and inhibiting mitochondrial permeability transition (mPT).

ADP/ATP antiporter ***c*** state to unspecific pore-forming, tensed-open uniporter state (***c'***) [70]. The peptidyl-prolyl *cis-trans* isomerase (PPIase) activity of the ANT-associated CypD may facilitate the above mentioned conformational changes of the ANT triggered by high $[Ca^{2+}]_m$. Thus, inhibition of the association of CypD to ANT by cyclosporin-A (CysA) or inhibition of the PPIase activity of the ANT-associated CypD by sanglifehrin-A (Sf-A) hinders the aforementioned conformational changes of the ANT and reduces substantially the Ca^{2+} sensitivity of the PTP [71;72]; both CysA and Sf-A are established inhibitors of PTP. Likewise, Mg^{2+} and other divalent cations (Mn^{2+}, Sr^{2+}) prevent pore-opening by competitively inhibiting Ca^{2+}-binding to ANT [73]. Protons (H^+) also compete for the same binding sites and thus, PTP is inhibited by acidification of the matrix pH below 7.0 [74] and optimal matrix pH for pore-opening is 7.4 [75]. Oxidative stress, peroxide and increased ROS production promotes PTP by oxidizing critical residues on the ANT, now believed to be the Cys^{160} [76], strengthening the notion that ANT is indeed involved in PTP formation. Moreover, adenine nucleotide depletion ([ATP]↓, [ADP]↓) and high phosphate (P_i), pyrophosphate (PP_i) concentrations (arsenate and vanadate as well) in the matrix enhance PTP opening by preventing adenine nucleotide binding to the ANT [56] and accordingly, the specificity and potency of different nucleotides as inhibitors of the PTP match their ability to be translocated by the ANT [77]. Amphipatic anions, such as free fatty acids (FFAs) produced by PLA_2 promote pore opening by affecting the lipid structure of the IMM [78] around the ANT, on the other hand amphipathic cations (e.g. sphingozine, trifluoperazine or spermine) favour pore closure [79]. Also, PTP is sensitive to the redox state of the cell: NADH is protective and substrates that increase the reduction of NAD^+ like pyruvate, α-ketoglutarate and glutamate are protective as well, while others that decrease the reduction like oxaloacetate or malonate are stimulators of pore opening [80]. Moreover, full-charged and resting membrane potential effectively prevents the pore-opening [81], parallel to the $\Delta\Psi_m$-

dependency of the antiporter state of ANT and a vide variety of pathophysiological effectors alters the threshold voltage at which opening occurs either closer to the resting potential (PTP inducers), or away from the resting potential (PTP inhibitors) [82].

1.2.4. Contribution of Cyclophilin-D to PT

Cyclophilin-D (CypD) is an 18 kDa matrix protein exhibiting peptidyl-prolyl *cis-trans* isomerase activity (PPIase) that is encoded by the nuclear gene *Ppif* [83]. CypD appears in both structural models of the PT pore mentioned in **Section 1.2.2**, being the target for the inhibitory effect of the immunosuppressant cyclosporine-A (CysA) on MPTP. Likewise, the PPIase activity of CypD appears to facilitate the conformational changes of the ANT (or PiC) molecule when forming the non-selective megachannel of PT [71;84] triggered by high loads of Ca^{2+}. The importance of the Ca^{2+}- and ROS-dependent PPIase activity of CypD in the initiation of PTP has been further supported by the use of the non-immunosuppresive CypD antagonists Sanglifehrin A (Sf-A) and Debio-025 [71;85;86]. The contribution of CypD to PTP formation was confirmed by experiments in which the *Ppif* gene encoding CypD was knocked out [87-90]. These mice do not show a severe phenotype: enchanced anxiety, avoidance behaviour, occurance of adult onset obesity [91] and a defect in platelet activation and predisposition for thrombosis [92]. CypD knockout mice exhibited lower sensitivity to focal cerebral and liver ischaemia, or in myocardial ischaemia/reperfusion and muscular dystrophy models [87-89;93-96]. Mitochondria from *Ppif* $^{-/-}$ mice were shown to be resistant to Ca^{2+} and oxidative stress-induced PTP and cell death, behaving identically to mitochondria from WT mice treated with CysA or Sf-A [87-90]. The loss of CypD did not prevent permeability transition, but increased substantially the load of stimuli necessary before pore opening occurred confirming the hypothesis, that MPTP opening involves a conformational

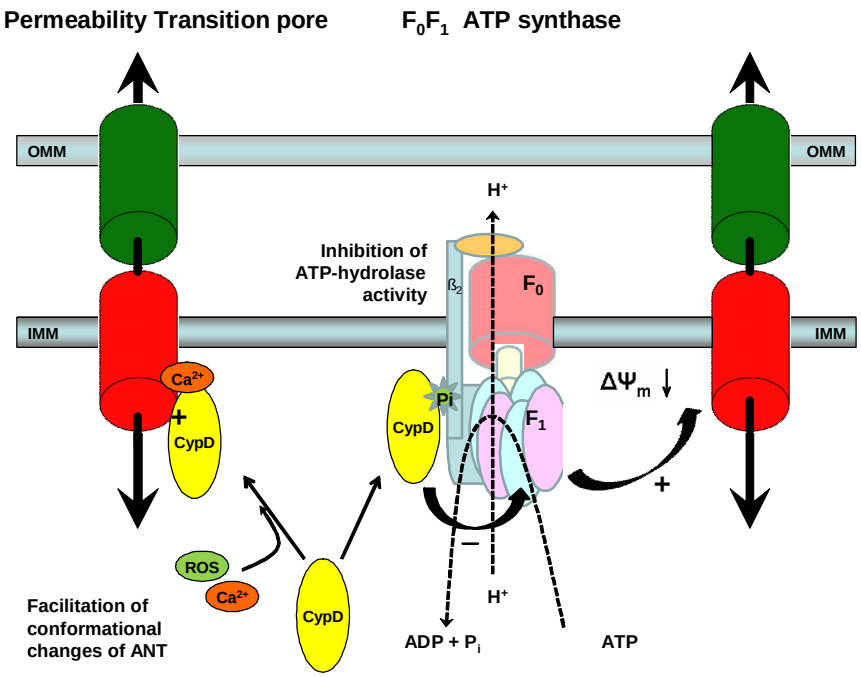

Figure 2. Direct and indirect promotion of PTP by cyclophilin-D (CypD).
Pi denotes the activating P_i-binding site

change in a membrane protein that is triggered by calcium and facilitated by CypD, but can occur in the absence of CypD if sufficient stimulus is given [97].

The physiological role of CypD remains unclear. However, apart from the high Ca^{2+}-induced binding to ANT, CypD has been shown recently to bind to the lateral stalk of the F_0F_1-ATP synthase as well (**Figure 2)** in a phosphate-dependent manner [98]; and it has been proposed that ablation of CypD or CysA treatment unmasks an inhibitory P_i binding site, rather than causing direct PTP inhibition [99] (reviewed in [100]). The absence of functional CypD leads to the disinhibition of the F_0F_1-ATP synthase resulting in accelerated ATP synthesis and hydrolysis rates [98;100]. Also, it has been postulated, that inorganic phosphate (P_i) may in fact be the true inhibitor of PTP acting on a binding site on F_1 masked by functional CypD [98-100]. The different factors that favour P_i binding to this site (*pmf* or preserved membrane potential, high [P_i], high [Mg^{2+}], acidic pH) are strikingly similar to the inhibiting factors of PTP (see **Section 1.2.3** and **Table 1**). Altogether,

the activity of CypD leads to PTP in two converging ways: one is the direct binding of CypD to ANT triggered by Ca^{2+} overload, facilitating it's conformational change to the pore-forming tensed open state and secondly, CypD inhibits the ATP hydrolase activity of the reversed ATP synthase by occupying a P_i binding site on the F_1 subunit, thus preventing the salvage of membrane potential, favoring PTP indirectly [100] (**Figure 2**).

Furthermore, the studies with CypD KO mice also converged to the conclusion that CypD mediated MPTP regulates some forms of necrotic, but not apoptotic death, a notion originally suggested by the group of Crompton and colleagues [101]. The complex contribution of CypD to brain-specific mitochondrial permeability transition induced by Ca^{2+} is demonstrated in [102] and **Section 4.1** of the present thesis.

1.3. NAADP and Ca^{2+} mobilization

Mitochondrial functions are fundamentally affected by cytosolic signalling events. At the ER-mitochondrial junctions, the formation of high Ca^{2+} microdomains has been detected [6;14;29-31], which constitutes a tangible link between cytosolic Ca^{2+} signalization and mitochondrial Ca^{2+} homeostasis, as described in Section 1.1.1. This section is devoted to one of the major pathways of Ca^{2+} mobilization from intracellular organelles upstream from the Ca^{2+}-related modulation of mitochondrial functions (e.g. regulation of matrix enzymes and initialization of PTP).

Understanding of the regulation of intracellular Ca^{2+} release and its relationship to extracellular stimuli were greatly broadened by the discovery of the inositol-1,4,5-trisphosphate ($InsP_3$) signalling pathway [1;2]. Although $InsP_3$ appears to operate as a ubiquitous intracellular messenger for Ca^{2+} mobilization, numerous studies indicate that additional Ca^{2+} release mechanisms operate in many cells and are regulated by a family of pyridine nucleotide metabolites [103-107]. The first indication for this concept came from the pioneering work of Lee and colleagues who showed that β-NAD^+ and β-$NADP^+$ could trigger Ca^{2+} release from sea urchin egg microsomal fractions by a mechanism apparently independent of $InsP_3$ [103]. Subsequently, the structure of the active metabolites has been determined, one of them being cyclic adenosine disphosphate ribose (cADPR) [108]. The Ca^{2+} mobilizing effect of β-$NADP^+$ was shown to be due to a contaminant of commercially available β-$NADP^+$ identified as nicotinic acid adenine dinucleotide phosphate (NAADP) [109]. Ca^{2+} release by both β-NAD^+ and β-$NADP^+$ appeared to operate via separate Ca^{2+} release mechanisms which were distinct from those gated by $InsP_3$, since $InsP_3$ showed homologous desensitization without affecting Ca^{2+} release by activators of the other two mechanism [108].

1.3.1. Structure of NAADP

NAADP is a simple derivative of $NADP^+$, with the only modification being the conversion of the amide of the nicotinamide group to a carboxyl group (**Figure 3**). In fact, the only difference between NAADP and $NADP^+$ is the substitution of an NH_2 of the amide moiety in $NADP^+$ with an OH^- of the carboxyl group in NAADP. The two compounds differ by only one mass unit and have identical proton NMR and UV spectra [109].

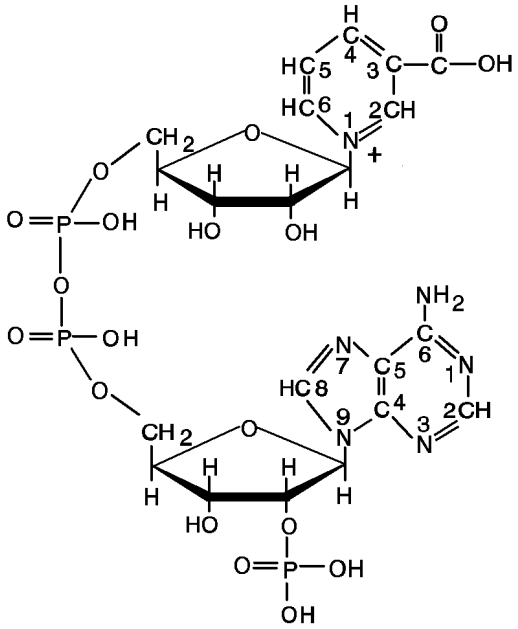

Figure 3. Structure of NAADP.

1.3.2. Ca^{2+} release activity of NAADP in mammalian cell systems

The first mammalian cell, in which NAADP was shown to be potent in mobilizing Ca^{2+} from internal stores, was the mouse pancreatic acinar cell in whole-cell patch configuration and whole-cell Ca^{2+}-activated current-detection [110]. In pancreatic acinar cells, what was immediately striking is the potency of NAADP compared to other Ca^{2+} mobilizing messengers: nanomolar concentrations of NAADP were effective, whereas micromolar concentrations of $InsP_3$ or cADPR are needed to evoke such responses. Curiously, higher concentrations of NAADP produced no discernible response. Generally, application of supra-threshold concentrations of NAADP in mammalian cells desensitizes the pathway to any further NAADP stimulation [111-115]

and in contrast to the sea urchin egg model, the NAADP receptor desensitization by sub-threshold doses of NAADP has only been reported in rat liver microsomes [116]. Quite remarkably, the effects of NAADP in pancreatic acinar cells were blocked by heparin or 8-NH_2-cADPR, specific antagonists of $InsP_3$ and cADPR receptors, respectively [111]. An attractive hypothesis was put forward by Cancela, Charpentier & Petersen to explain this finding. Namely, NAADP provides a trigger release of Ca^{2+} that is subsequently propagated by $InsP_3$ and ryanodine receptors by Ca^{2+}-induced Ca^{2+} release [111]. Inactivation of NAADP receptors by high concentrations of NAADP has little effect on responses to $InsP_3$ and cADPR, adding further support to the idea that NAADP receptors activate upstream of $InsP_3$ and ryanodine receptors [111].

Similar Ca^{2+} release activity was seen with different techniques from a variety of mammalian cell types, such as brain- [117], heart- [118], kidney- [119], liver microsomes [116] (see also **Section 4.2** of the present thesis), T-lymphocytes [120], skeletal muscle [121], microsomes derived from mammalian cell lines [122] and plant cells [114]. The pattern of NAADP-mediated Ca^{2+} release appeared to be biphasic, with an initial rapid release followed by a sustained but slower phase of release [116;118]. Similarly to the invertebrate systems, the NAADP-induced Ca^{2+} release was Ca^{2+}-independent in a wide range of pCa and pH-independent between pH 6.8 and 8.0 [116;118]. On the other hand, the activity of a lysosomal NAADP-reactive Ca^{2+} channel was highly potentiated by acidification of the medium in single-channel recordings [123].

1.3.3. The NAADP receptor

In sea urchin eggs, one big step towards the identification of the NAADP receptor has been made by solubilizing a protein that binds NAADP irreversibly and with high affinity [124]. The molecular weight

of the solubilized NAADP-binding protein (~471 kDa, presumably a tetramer of 120 ± 2 kDa subunits) was substantially lower than that of the $InsP_3R$ (~1000 kDa, tetramer of ~300 kDa subunits) and RyR (~2000 kDa, tetramer of ~560 kDa subunits) [125].

Biochemical, pharmacological and physiological evidences support the existence of a novel intracellular receptor [126]. First of all, [^{32}P]NAADP binding studies showed that NAADP binds to specific binding sites in sea urchin egg homogenates [127;128], as well as in microsomes preparated from heart [118] and brain [129], and also in MIN6 insulinoma cells [113]. In brain and heart microsomes and MIN6 cells, [^{32}P]NAADP binding was proven to be reversible [113;118;129], while in sea urchin eggs [^{32}P]NAADP binding appears to be essentially irreversible [127]. The irreversible nature of NAADP receptor binding may contribute to the unusual, U-type self-desensitization of the NAADP-mediated pathway in sea urchin eggs [106;127;130] discussed previously. Neither Ca^{2+}, nor changes of the pH can displace the receptor binding of NAADP [131]. On the other hand, NAADP displays a high apparent affinity for the type 1 RyR in electrophysiological and biochemical experiments in some mammalian cells, e.g. Jurkat T-lymphocytes [120;132;133], skeletal muscle HSR vesicles [121] and the nuclear envelope of pancreatic acinar cells [134]. The EC_{50} (~30nM) of NAADP is comparable to that described for Ca^{2+} release in these systems [120;121;132;134], and inhibition of RyRs by RuRed concentration-dependently antagonized the Ca^{2+} mobilization by NAADP [120;121]. Meanwhile, the type 2 RyR from dogs, which represents the cardiac isoform, was also found to respond to NAADP in single-channel recordings [135]. However, it is important to underline that the interaction between NAADP and the RyRs (directly or via an accessory protein) does not rule out the existence of a genuine NAADP receptor but rather emphasizes the complexity of NAADP action [136].

Moreover, direct evidence has been provided with planar lipid bilayer technique that an NAADP-sensitive Ca^{2+} channel is present in rat

liver lysosomes [123]. The NAADP-induced activation of these lysosomal Ca^{2+} channels was markedly attenuated by blockade of TRP-ML1 (transient receptor potential-mucolipin 1) protein by anti-TRP-ML1 antibody, which are different from RyR and $InsP_3R$ Ca^{2+} release channels on the ER/SR [123].

The year 2009 has witnessed a major breakthrough in the search for the NAADP receptor: the two-pore cation channel 2 (TPCN) expressed on the acidic Ca^{2+} stores has fulfilled the basic criteria for being the long sought native lysosomal receptor for NAADP [137;138]. Nanomolar concentrations of NAADP trigger robust Ca^{2+} release from HEK293 cells transfected with TPCN2 which can be desensitized by the application of micromolar NAADP and abolished by pharmacologically blocking lysosomal Ca^{2+} storage capacity [137]. TPCN2 has been demonstrated to localize on lysosomes [137;138] and binding studies confirmed that TPCN2 enriched membranes have two affinities to NAADP with K_d~5nM and ~7μM [138] comparable with other mammalian preparations [113;118;129].

1.3.4. The NAADP/Ca^{2+} signalling pathway

The Ca^{2+} stores activated by NAADP have been extensively studied and it appears that NAADP directly releases Ca^{2+} from a wider variety of intracellular organelles than $InsP_3$ and cADPR. Alongside the ER/SR, which is the major target for $InsP_3$ and cADPR, NAADP mobilizes Ca^{2+} from the nuclear envelope (alongside $InsP_3$ and cADPR) [134] and from the acidic Ca^{2+} stores (e.g. lysosomes, reserve granules) in various cell types such as sea urchin eggs, smooth muscle cells, glial cells, mouse pancreatic acinar cells) [139-142] and insulin-containing vesicles in pancreatic beta cells [143]. The acidic Ca^{2+} stores sequester Ca^{2+} via a SERCA/thapsigargin-independent mechanism which is a combination of bafilomycin-sensitive V-type H^+-ATPase and a Ca^{2+}/H^+-exchanger (**Figure 4 A**) [139] and the acidic Ca^{2+} stores can be

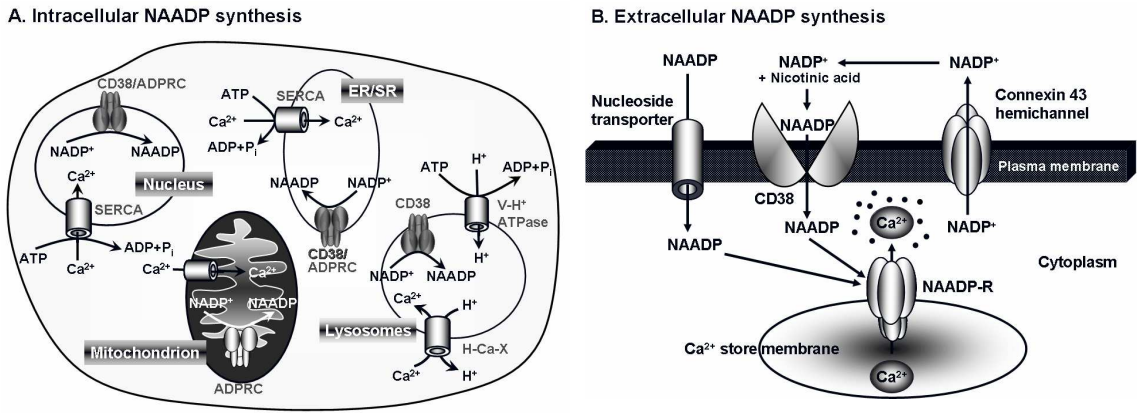

Figure 4. (A) Intracellular localizations of ADPRC/CD38 activity and NAADP synthesis and (B) models for the synthesis of NAADP extracellularly by the ectoenzyme, CD38 or in the lysosomal compartment by internalization of CD38.

selectively disrupted with GPN (glycyl-phenylalanyl-naphtylamide) [144]. Moreover, the intraluminal pH of rat liver lysosomes (pH_L) has recently been shown to rise in accordance with Ca^{2+} release by NAADP [145] that may be due to Ca^{2+} re-uptake into lysosomes via the Ca^{2+}/H^+-exchanger [145].

Likewise, bafilomycin A1 and GPN are able to abolish selectively the NAADP-induced Ca^{2+} signalling in the forementioned cell types [141;143;146;147]. In addition to acidic organelles, the NAADP-mediated Ca^{2+} response incorporates Ca^{2+} release via direct activation of RyRs on the ER/SR in heart, skeletal muscle and T-cells [120;121;135] and/or Ca^{2+} entry described in both invertebrates (e.g. starfish oocytes) [148] and in mammalian T-lymphocytes [133]. Direct activation of RyRs by NAADP was confirmed on isolated RyRs reconstituted in lipid bilayers from rabbit skeletal muscle (RyR1) [121] and dog cardiac microsomes (RyR2) [135].

Cells thus possess multiple Ca^{2+} stores and interaction between these pools is crucial for the adequate Ca^{2+} response to different extracellular signals. In a wide range of cells, the two pool model or trigger hypothesis is best suited to depict the Ca^{2+} signalling by NAADP, cADPR and $InsP_3$. In this model, NAADP activates the acidic Ca^{2+} stores and evokes localized Ca^{2+} signals that act as a trigger [149;150]. These

localized Ca^{2+} signals are then amplified and propagated by $InsP_3Rs$ and RyRs on the ER by CICR [110;149-151]. This model accounts for the finding that in many cells, the localized NAADP-induced signals persist in the presence of $InsP_3Rs$ and RyR antagonists or thapsigargin, but are abolished by bafilomycin A1 or GPN [139;141;143;146;147]. On the other hand $InsP_3Rs$ and RyR antagonists are able to abolish the NAADP-induced Ca^{2+} oscillations and global waves in these cells [141;146;147]. Alternatively, in those systems where NAADP was shown to interact directly with the RyRs expressed on the ER/SR (heart and skeletal muscle [121;135], T-lymphocytes [120] and nuclear envelope of pancreatic acinar cells [134]) a single-pool model can be applied. Likewise, the effects of NAADP are completely abolished by inhibitors of RyR in these systems [120;121;134;135].

An important step towards the classification of NAADP as second messenger, i.e. the measurement of the changes in NAADP levels in response to extracellular stimuli has been solved by using a radioreceptor assay with the NAADP binding protein from sea urchin eggs [113;142;147;152-154]. NAADP levels have been shown to rise in sea urchin sperm during activation before fertilization [152;154] and in sea urchin eggs, the synthesis of NAADP was potentiated by rising levels of cAMP, while production of cADPR was very sensitive on rises of intracellular cGMP levels [155]. In mammalian smooth muscle cells, the application of endothelin-1 (ET-1) provoked considerable NAADP-production [147] and pancreatic acinar cells responded to the gut-peptide cholecystokinin (CCK) with promptly elevated concentrations of NAADP [142]. Moreover, the intracellular NAADP concentration rises in response to glucose in pancreatic beta cells [113].

The debate is now strong on the issue of the localization of NAADP-production inside or outside the cells. In one model, translocation (endocytosis) of CD38 and compartmentalization of nicotinic acid and $NADP^+$ into the acidic calcium-stores could provide an appropriate environment for the synthesis of NAADP in vivo [156]. An

other tentative model to resolve the paradox on the synthesis of an intracellular messenger on the cell surface by an ectoenzyme has been elaborated in the case of cADPR [157;158]. In this model, NAD^+ (and related pyridine dinucleotides, maybe $NADP^+$ as well) can leave the cell via connexin 43 hemichannels [157] and then converted to cADPR by CD38 extracellularly. cADPR is able to re-enter the cells via either a transporter formed by the CD38-dimer or by nucleoside transporters [158]. A similar influx of NAADP from the extracellular space into astocytes has been revealed through connexin hemichannels and gap junctions (and additionally by pinocytosis) [140;159] indicating that NAADP may also act as a paracrine signalling molecule [140] (**Figure 4 B**). Nonetheless, we can not exclude the possibility of intracellular NAADP synthesis by CD38, that has been shown to exist in intracellular localizations, such as mitochondria [160], ER and the nuclear envelope [161], or even by a novel intracellular CD38-independent $NADP^+$-converting enzyme as demonstrated in CD38 -/- mice [162] (**Figure 4 A**).

Finally, we are going to put together the pieces of the NAADP/Ca^{2+} signalling pathway. In sea urchin sperm, NAADP-production bursts during activation by contact with egg jelly and the cortical reaction in the oocyte (zygote) after fertilization is mediated by NAADP [154]. One way of coupling the extracellular signals to NAADP synthesis by ADPRCs may be via the cAMP-pathway in sea urchin oocytes [155]. In pancreatic acinar cells, CCK-receptors recruit both the cADPR- and NAADP-mediated Ca^{2+} signalling pathway, while bombesin activates RyRs/cADPR and acetylcholine (ACh) induces the $InsP_3Rs$ enabling the cell to differentiate between different extracellular stimuli [110;149;163-165]. A recent study showed that bile acids may induce complex intracellular Ca^{2+} signalling in pancreatic acinar cells via the NAADP-mediated pathway, which acts as a triggering signal [166]. This may be an important link between biliary reflux and pancreatic acinar cell necrosis [166]. In MIN6 insulinoma cells and pancreatic beta cells, NAADP plays a central role in the glucose-induced insulin secretion and

ATP, cAMP or glucose itself might up-regulate NAADP synthesis [113]. In arterial smooth muscle cells, endothelin-1 (ET-1), but not $PGF_{2\alpha}$ is coupled with NAADP-dependent Ca^{2+} signalling [147] giving an other good example for differentiation between extracellular stimuli. In T-lymphocytes, T-cell receptor/CD3 activation and subsequent Ca^{2+} signalling is medited by NAADP [120] and in the nervous system NAADP potentiates neurit outgrowth [146] and neurotransmitter release [167]. Thus, the NAADP-responsive cells are as widespread among the living beings as the NAADP-mediated functions in the living cells [168].

2. Aims and objectives

The primary aim of the present thesis was to clarify the modulatory role of cyclophilin-D in the Ca^{2+}-induced permeability transition and it's relation to the bioenergetic state of mitochodria. We first verified that substrate-starved mitochondria are indeed more susceptible to Ca^{2+}-induced permeability transition in our experimental settings using a 3-step Ca^{2+}-addition protocoll, and that genetic deletion of CypD provides similar, overridable protection to that of cyclosporin-A in wild-type, substrate-starved mitochondria. Also, we performed paralell recordings of swelling and Ca^{2+} uptake into mitochondria in the presence of Ru360 or an uncoupler. These results rose the question whether high Ca^{2+} acts on the surface of mitochondria or is entering mitochondria by a RuRed/Ru360-independent pathway. To decide between these possibilities, we challanged *in situ* mitochondria with Ru360 and Ruthenium Red and recorded Ca^{2+} uptake capabilities. Next, we clarified the contribution of the different complexes of the electrone transport chain to Ca^{2+}-induced swelling by using inhibitors of Complex I, III and IV. Finally, we demonstrated the diverse effect of the ablation of cyclophilin-D on the swelling of *in situ* mitochondria of neurons and astrocytes. Moreover, we showed that the deletion of cyclophilin-D not only delays initial swelling of neuronal mitochondria induced by excitotoxicity (glutamate-glycine), but it also renders neurons less susceptible to delayed calcium deregulation.

On the other hand, in regard to cytosolic Ca^{2+} signalization, the main objective of our work was to establish NAADP as a distinct pathway for Ca^{2+} release in heart microsomes. Firstly, we defined the actively loaded microsomal Ca^{2+} store to be thapsigargin-, but not bafilomycin A1-sensitive. In the next step, we verified that NAADP was indeed active in mobilizing Ca^{2+} from rat heart microsomes and we compared the Ca^{2+} releasing potential of NAADP to those of $InsP_3$ and cADPR. Also, we showed the lack of cross-desensitization between

NAADP, cADPR and $InsP_3$ as an evidence for separate receptors for each Ca^{2+}-mobilizing second messengers. Focusing on the properties of the NAADP-dependent Ca^{2+} release, we provided a dose-dependence curve, as well as pH- and pCa-dependence curves for the NAADP-induced Ca^{2+} efflux from heart microsomes. We showed for the first time in vertebrate tissues the unique inactivation pattern of the NAADP-mediated Ca^{2+} release, where 'per se' non-Ca^{2+}-mobilizing doses of NAADP are able to abolish the effect of a saturating quanta of NAADP. Furthermore, we incubated pre-loaded microsomes with thapsigargin and bafilomycin A1 to support the notion that the one-pool model is applicable for the Ca^{2+} release from the microsomal Ca^{2+} stores. Finally, by demonstrating the pharmacological properties of the NAADP-induced Ca^{2+} efflux, we provided strong evidence for NAADP being an independent mediator from $InsP_3$ and cADPR in heart microsomes.

3. Materials and methods

3.1. Mitochondrial and microsomal preparations

3.1.1. Isolation of brain mitochondria from WT and CypD KO mice - C57Bl/6

WT and KO for cyclophilin-D littermate mice were a kind gift from Drs. Nika Danial and Anna Schinzel, from Howard Hughes Medical Institute and Dana-Farber Cancer Institute, Harvard Medical School. Mice were cross-bread for 8 generations prior to harvesting brain tissues from WT and KO age-matched animals for the purpose of mitochondrial isolation and culturing of neurons and astrocytes. Non-synaptic brain mitochondria from adult male WT and KO for CypD mice (aged 87-115 days) were isolated on a Percoll gradient as described previously [169] with minor modifications detailed in [170]. All animal procedures were carried out according to the local animal care and use committee (Egyetemi Állatkísérleti Bizottság) guidelines.

3.1.2. Preparation of rat liver microsomes

Liver microsomes were prepared as described previously by Fleishner and Kraus-Friedmann [171]. Briefly, Sprague-Dawley rat liver was homogenised in an ice-cold medium of 0.32 M sucrose, 20 mM MOPS-buffer (pH 7.2), 0.5 mM EGTA also containing 1 mM dithiothreitole (DTT) and 0.2 mM phenylmethylsulfonyl fluoride (PMSF) as protease inhibitors and centrifuged at 2000x*g* for 15 minutes at 4 °C. The supernatant was centrifuged at 15,000x*g* for 45 minutes, and the resulting supernatant was collected and further centrifuged at 100,000x*g* for 90 minutes. Finally the pellet was resuspended in a solution containing 0.32 M sucrose, 20 mM MOPS (pH=7.2), 1 mM DTT and 0.2 mM PMSF. Protein concentration was set for ~20 mg/ml which was measured by the Lowry assay using bovine serum albumine as standard.

The samples were frozen in liquid nitrogen and stored at -80 °C until required.

3.2. Mitochondrial membrane potential ($\Delta\Psi_m$) determination

$\Delta\Psi_m$ was estimated using fluorescence quenching of the cationic dye safranine O, because of its accumulation inside energized mitochondria [172]. Mitochondria (1 mg) were added to 2 ml of an incubation medium containing 120 mM KCl, 20 mM Hepes (acid), 10 mM potassium phosphate, 1 mM $MgCl_2$, 0.005 mM EGTA, 5 mM potassium glutamate, 5 mM potassium malate, 0.001 mM cyclosporine A, 0.05 mM AP_5A, 0.5 mg/ml BSA and 5 µM safranine O (pH 6.8 or pH 7.8). Fluorescence was recorded in a Hitachi F-4500 spectrofluorimeter (Hitachi High Technologies, Maidenhead, UK) at a 5 Hz acquisition rate, using 495 and 585 nm excitation and emission wavelengths, respectively. Experiments were performed at 37 °C. To convert safranine O fluorescence into millivolts (mV), a voltage–fluorescence calibration curve was constructed. To this end, safranine O fluorescence was recorded in the presence of 2 nM valinomycin and stepwise increasing $[K^+]$ (in the 0.2–120 mM range), which allowed calculation of $\Delta\Psi_m$ by the Nernst equation, assuming a matrix $[K^+]$ of 120 mM [172].

3.3. Ca^{2+} uptake of isolated mitochondria

Mitochondrial-dependent removal of medium Ca^{2+} was followed using the impermeant hexapotassium salt of the fluorescent dye Calcium Green 5N (CaGr) (Molecular Probes, Portland, OR, USA). CaGr (500 nM) was added to a 2 ml medium containing mitochondria (0.125 mg/ml) and 120 mM KCl, 10 mM Tris, 5 mM KH_2PO_4, 1 mM $MgCl_2$, pH 7.6. Substrates were added where indicated. All experiments were performed

at 37 °C. Fluorescence intensity was measured in a Hitachi F-4500 fluorescence spectrophotometer (Tokyo, Japan) using 517 nm excitation and 535 nm emission wavelengths.

3.4. Measurement of mitochondrial swelling

Swelling of isolated mitochondria was assessed by measuring light scatter at 520 nm in a GBC UV/VIS 920 spectrophotometer. Mitochondria were added at a final concentration of 0.125 mg/ml to 2 ml of medium containing 120 mM KCl, 10 mM Tris, 5 mM KH_2PO_4, 1 mM $MgCl_2$, pH 7.6. Substrates were added where indicated. At the end of each experiment, the non-selective pore-forming peptide alamethicin (40 µg) was added as a calibration standard to cause maximal swelling. All experiments were performed at 37 °C.

3.5. Matrix Ca^{2+} imaging of isolated mitochondria

Visualization of isolated mitochondria under epifluorescence imaging (100x1.3 NA) was achieved by loading mitochondria with Fura 2 AM (8 µM for 20 min at 30 °C). Mitochondria were diluted to 1 mg/ml, and 5 µl was dropped on a coverslip, allowed to stand for 4 minutes prior to starting the perfusion. Image sequences (10 s/ratio frame, 50 ms exposure time, 2 × 2 binning) were acquired using a Micromax cooled digital CCD camera (Princeton Instruments) mounted on a Nikon Diaphot 200 inverted microscope (Nikon Corp., Tokyo, Japan). Image acquisition was controlled by Metafluor 3.5 (Universal Imaging Corp., West Chester, PA, USA). The perfusate (50 ml/h flow rate) was temperature controlled at 37 °C at the side of the recording. The composition of the perfusate was 120 mM KCl, 10 mM Tris, 5 mM KH_2PO_4, 1 mM $MgCl_2$, pH 7.6.

3.6. Determination of ANT content of mitochondria

The ANT content of mitochondria was estimated from titration curves obtained by stepwise addition of cATR to isolated mitochondria during state three respiration, as described by Schonfeld [173].

3.7. Active loading of microsomes with Ca^{2+} and Ca^{2+} release assay

Ca^{2+} uptake and release were measured using $^{45}Ca^{2+}$ isotope to detect Ca^{2+} movements. The microsomes were diluted in a solution of 150 mM KCl, 20 mM MOPS (pH 7.2), 0.5 mM $MgCl_2$, 10 µM Ca^{2+}. In each experiment, 20-40 nCi $^{45}CaCl_2$ was used per assay point. The Ca^{2+} uptake was started by injecting 1 mM of ATP in the solution at room temperature. Ca^{2+} release was preformed by adding 100 µM EGTA in the presence or absence of the Ca^{2+} releasing agents (10 µM $InsP_3$, 10 µM cADPR and 10 µM NAADP). The $^{45}Ca^{2+}$ remaining in the vesicles was determined by filtration of 0.5 ml microsomes through a nitrocellulose Millipore filter (HAWP, 0.45 µm pore size) under vacuum. The filters were washed with 5 ml of quench solution (150 mM KCl, 20 mM MOPS (pH 7.2), 10 mM $MgCl_2$ and 1 mM $LaCl_3$) in order to lower the rate of unspecifically bound radioactivity. The radioactivity retained on the filter was measured by standard scintillation counting.

3.8. Passive loading of microsomes and Ca^{2+} release

Liver microsomes were passively loaded with 5mM $^{45}CaCl_2$ (20-40 nCi per assay point) by incubation for at least 5 hours in an ice-cold medium containing 150 mM KCl, 20 mM MOPS (pH 7.2), $^{45}Ca^{2+}$ and 5 mM Ca^{2+}. Passive loaded vesicles were diluted 10-fold into a Ca^{2+} releasing medium containing 150 mM KCl, 20 mM MOPS (pH 7.2) and

500 µM of EGTA to adjust pCa to 6 at room temperature and Ca^{2+} releasing agonists. The Ca^{2+} release was stopped by 5-fold dilution with the same quench solution described above, then the samples were filtrated through Millipore filters and washed by 5 ml of quench solution. The retained radioactivity was measured by standard scintillation counting.

3.9. Reagents and statistics

Standard laboratory chemicals, oligomycin, stigmatellin, AP_5A, ADP, safranine O, cyclosporin A, nigericin, potassium acetate (prepared from acetic acid and KOH titrated to pH 7.2), methylamine and valinomycin were from Sigma (St Louis, MO, USA). CaGreen-5N was from Invitrogen (Carlsbad, CA, USA). Ru360 was from Calbiochem (San Diego, CA, USA). SF 6847 was from Biomol (catalog number EI-215; BIOMOL GmbH, Hamburg, Germany). All mitochondrial substrate stock solutions were dissolved in double distilled water and titrated to pH 7.0 with KOH. ADP was purchased as a potassium salt of the highest purity available, and titrated to pH 6.9.

Data are presented as mean ± standard error of the mean; significant differences between two sets of data were evaluated by ***t***-test, with $P < 0.05$ considered to be significant, and if there were more than two groups of data, a one-way ANOVA followed by Tukey's post hoc analysis was performed, with $P < 0.05$ considered to be significant. Wherever single graphs are presented, they are representative of at least three independent experiments.

4. Results and discussion

4.1. Complex contribution of cyclophilin-D in brain-specific mitochondrial permeability transition induced by Ca^{2+}

4.1.1. Effect of substrate availability on Ca^{2+}-induced PTP and modulation by cyclosporin A or genetic deletion of cyclophilin-D

Electrophoretic Ca^{2+} uptake for induction of PTP is allowed either in the presence of respiratory substrates or in a substrate-free medium containing KSCN; diffusion of the lipophilic SCN^- anion provides the driving force for electrophoretic Ca^{2+} accumulation [174;175]. However, in the original studies by Hunter and Haworth it was shown that PTP can be induced by Ca^{2+} in the absence of respiratory substrates [73;73], a phenomenon that has been subsequently reproduced [176-178], reviewed in [179]. Furthermore, it was also shown that substrates delay Ca^{2+}-induced PTP [176;177], in accordance to the Bernardi scheme elaborated above. To reproduce these findings for our studies, isolated brain mitochondria were challenged by $CaCl_2$, in the presence and absence of glutamate and malate, and light scattering was recorded spectrophotometrically at 520 nm. A three-pulse $CaCl_2$ protocol was used for this, and all subsequent similar experiments: 20 µM $CaCl_2$ was given at 100 sec, followed by 200 µM $CaCl_2$ at 300 sec and again at 500 sec. Orange lines appearing in **Figures 5**, **6**, and **8** represent traces obtained from WT mitochondria incubated in such conditions that reproduced the most pronounced swelling induced by CaC_2 (respective for each panel), but these mitochondria were not challenged by $CaCl_2$.

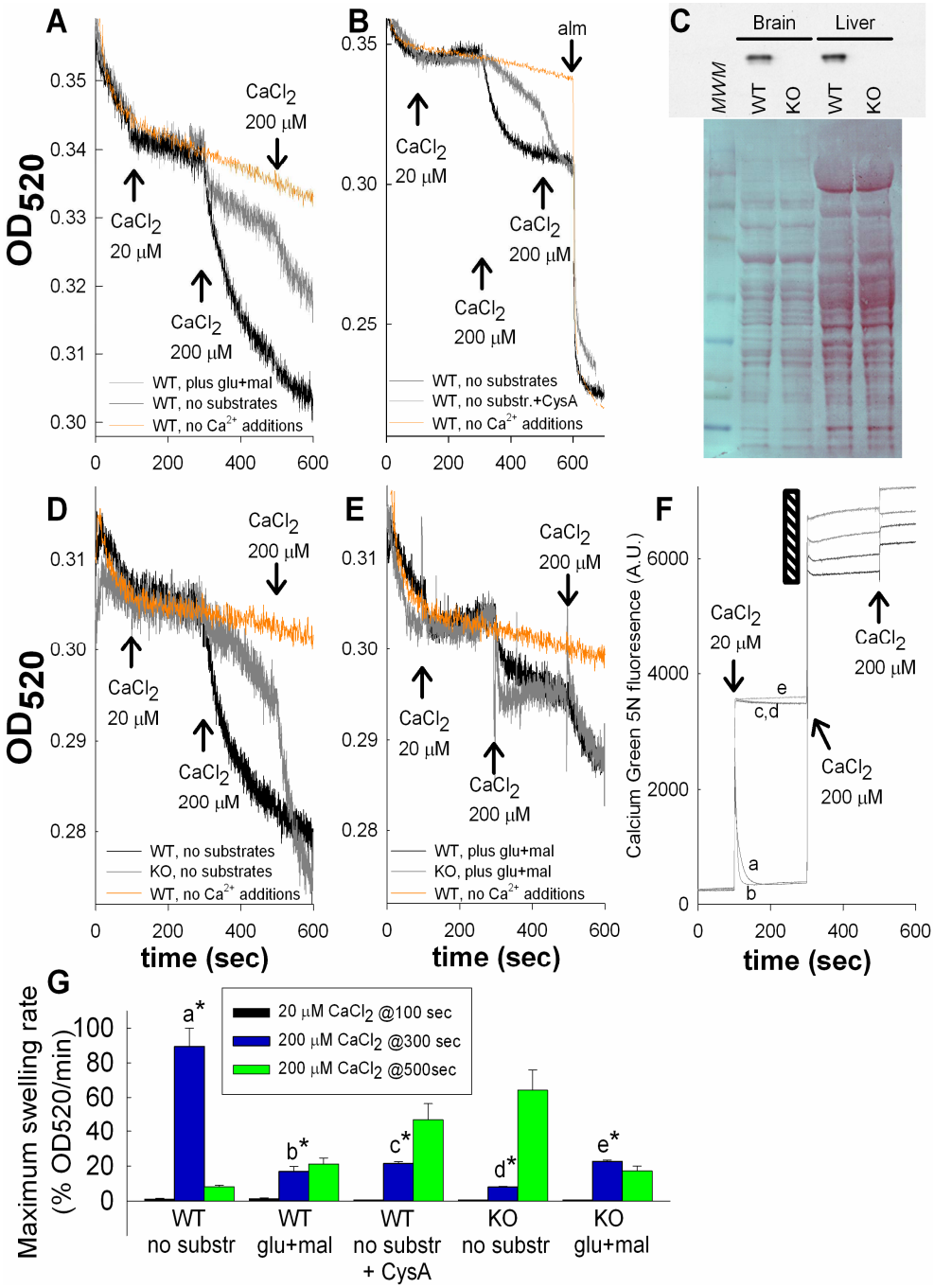

Figure 5. Effect of substrate availability on Ca^{2+}-induced PTP and modulation by cyclosporin A or genetic deletion of cyclophilin-D. **A**, **B**, **D**, **E**: Traces of light scatter recorded spectrophotometrically in mitochondrial suspensions at 520 nm during $CaCl_2$ additions at the concentrations indicated in the figures. Conditions are given in the panels. **C**: Western blot (upper panel) of brain and liver mitochondria from WT vs KO CypD mice probed for CypD immunoreactivity. Lower panel: Ponceau S staining of the same blot shown in the upper panel. MWM: Molecular Weight Marker. Panels **D** and **E** are aligned on the *y*-axis. Panels **A**, **D**, **E** and **F** are aligned on the *x*-axis. **F**: Mitochondrial Ca^{2+} uptake followed by Calcium Green 5N hexapotassium salt fluorescence (non-calibrated). The black stripped region is expanded on the *y*-axis, for the sake of clarity; *a*: WT, plus glutamate plus malate; *b*: WT, plus glutamate plus malate plus CysA; *c*: WT, no substrates; *d*: WT, no substrates plus CysA; *e*: WT, no substrates plus Ru360. Results are representative of at least 4 independent experiments. Panel **G** depicts the maximum swelling rates pooled from all individual experiments (expressed as percentage of swelling rate per minute and accounting for the condition producing the highest swelling rate as 'maximum') for each condition and after each Ca^{2+} pulse. Error bars represent S.E.M.; a is statistically significant from b, c, d, and e, $p<0.001$; d is statistically significant from e, $p<0.05$, one-way ANOVA on Ranks.

As shown in **Figure 5 A**, addition of 20 µM $CaCl_2$ to substrate-supplemented or substrate-starved brain mitochondria of wild type mice did not cause a decrease in light scatter; instead, a cessation in the baseline decrease in light scatter was observed. However, the subsequent 200 µM $CaCl_2$ pulse induced a large decrease in light scatter in substrate-starved but not substrate-supplemented mitochondria. The next 200 µM $CaCl_2$ pulse given at 500 sec did not induce any further changes in light scatter for the substrate-starved mitochondria, but it caused a minor change in substrate-supplemented mitochondria. As shown in **Fig. 5**, *panel B*, the effect of the first 200 µM $CaCl_2$ pulse was Cyclosporin A-sensitive, however, the second addition of 200 µM $CaCl_2$ overrode the protective effect of Cys A, consistent with the findings by Brustovetsky and Dubinsky [180]. In *panel B* the effect of the pore-forming peptide alamethicin is also shown, so that the extent of changes in light scatter induced by $CaCl_2$ can be better appreciated as compared to maximum changes. Subsequent experiments benefited from the availability of cyclophilin-D knock-out mice. We isolated mitochondria from the brains of WT and CypD-KO mice (see **Figure 5**, *panel C*). As shown in *panel D*, results obtained from substrate-starved mitochondria from CypD-KO mice were strikingly similar to those obtained from CysA-treated WT mice (*panel B*). The presence of substrates, however, did not provide additional protection in the CypD-KO mitochondria (*panel E*). Maximum swelling rates pooled from all experiments (expressed as percentage of swelling rate per minute and accounting for the condition producing the highest swelling rate as ‘maximum’) for each condition and after each Ca^{2+} pulse is shown in **Fig. 5**, *panel G*. These results are in accord to earlier reports on various types of mitochondria and conditions, showing that high-Ca^{2+} loads can induce PTP in the absence of substrates. In our hands, absence of substrates prevented isolated mitochondria from building a membrane potential of higher than -10 mV (not shown). At this $\Delta\Psi_m$ value, mitochondrial Ca^{2+} uptake is unfavorable [51]. Indeed, recordings of extramitochondrial Ca^{2+} by Calcium Geeen 5N revealed

that in the absence of substrates (**Figure 5**, *panel F*, traces *c*, *d*, and *e*) mitochondria were unable to perform Ca^{2+} sequestration, yet exhibited large changes in light scatter. Electron microscopy imaging of mitochondria that exhibited large changes in light scatter confirmed that this was due to swelling (not shown). We therefore considered the possibilities that Ca^{2+} was either inducing CypD-sensitive swelling by acting on an extramitochondrial site, or since high amounts of $CaCl_2$ were required, Ca^{2+} was entering mitochondria simply by a chemical gradient.

4.1.2. Effect of an uncoupler and/or inhibitors of the Ca^{2+} uniporter on mitochondrial Ca^{2+} uptake and light scatter

To address the site of action of Ca^{2+} on the light scatter, we pretreated mitochondria with the Ca^{2+} uniporter inhibitor, Ru360 [21]. As shown in **Figure 6 A**, WT mitochondria still exhibited high-Ca^{2+}-induced changes in light scatter in the presence of Ru360, at a concentration that was found to prevent the uptake of extramitochondrial Ca^{2+} (**Figure 5**, *panel F*, trace *e*). The lack of effect of Ru360 was also observed in the presence of Cys A (**Figure 5**, *panel A*), or when the effect of Ca^{2+} was compared in WT versus CypD-KO mitochondria (**Figure 6**, *panel B*). In order to depolarize mitochondria completely, 1 µM SF 6847 was added to the medium, and the effects of Ca^{2+} and Ru360 were recorded. As shown in **Fig. 6**, *panel C*, the presence of the uncoupler failed to afford extra protection against high-Ca^{2+} induced swelling. Furthermore, the presence of the uncoupler negated the protective effects of substrates in WT mitochondria (*panel D*). Maximum swelling rates pooled from all experiments (expressed as in **Figure 5**) for each condition and after each Ca^{2+} pulse is shown in *panel E* of **Figure 6**.

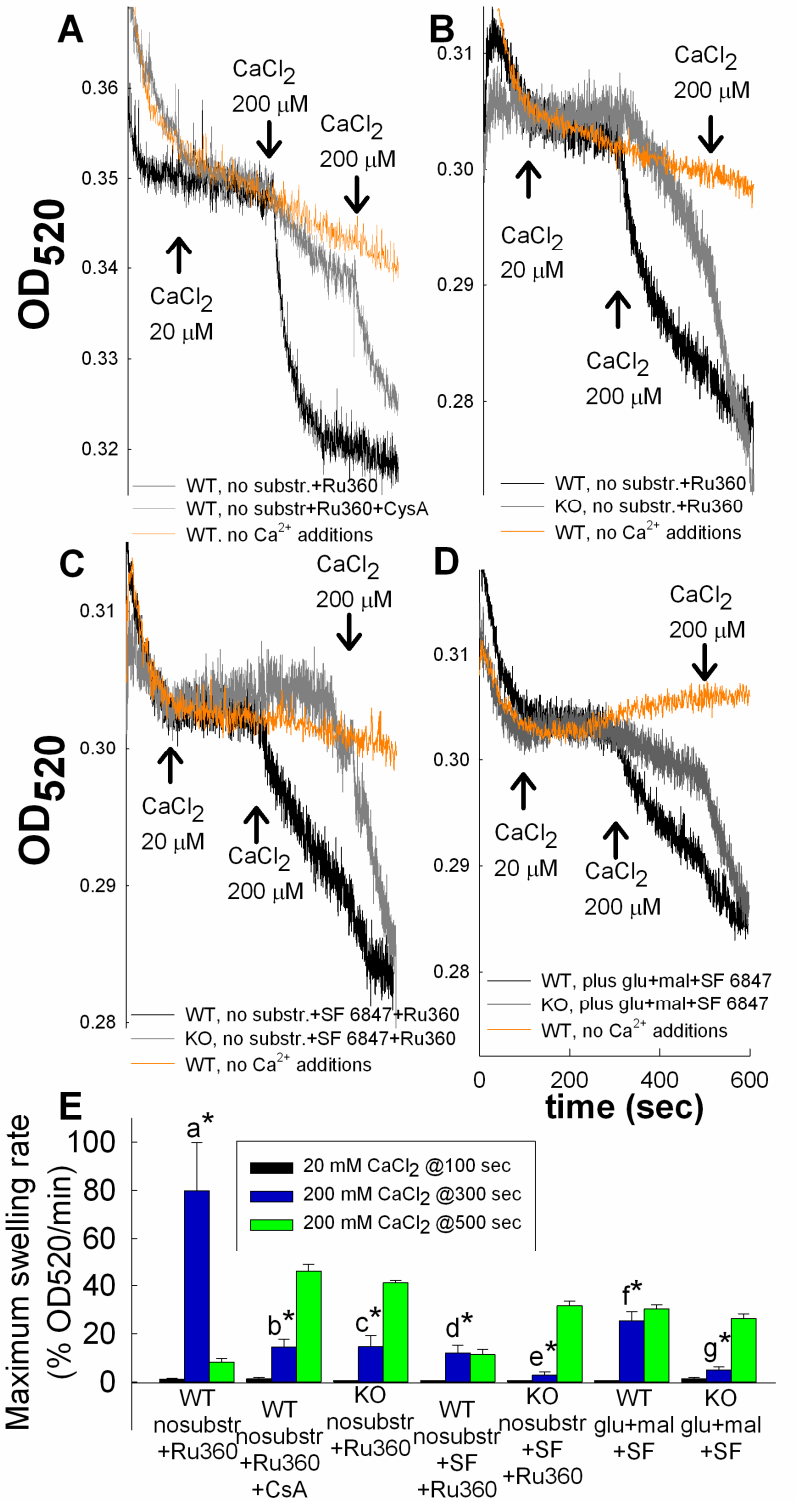

Figure 6. Effect of SF 6847 and/or inhibitors of the Ca^{2+} uniporter on mitochondrial Ca^{2+} uptake; modulation by Cyclosporin-A or genetic deletion of Cyclophilin-D. Traces of light scatter recorded spectrophotometrically at 520 nm during $CaCl_2$ additions at the concentrations indicated in the figures, to mitochondrial suspensions. Conditions of the suspensions are given in the panels. All panels are aligned on the *x*-axis. Results are representative of at least 4 independent experiments. Panel **E** depicts the maximum swelling rates pooled from all individual experiments (expressed as in **Figure 5**) for each condition and after each Ca^{2+} pulse. Error bars represent S.E.M.; a is statistically significant from b, c, d, e, f, and g, $p<0.001$; d is statistically significant from e, $p<0.05$, one-way ANOVA on Ranks.

4.1.3. Effect of Ca^{2+} uniporter inhibitors on mitochondrial matrix Ca^{2+} accumulation of isolated mitochondria imaged under wide-field epifluorescence

The failure of Ru360 to protect against the Ca^{2+}-induced large changes in light scatter shown in **Figures 6 A** and **6 B** could be explained by assuming that Ca^{2+} acted on the extramitochondrial side. To

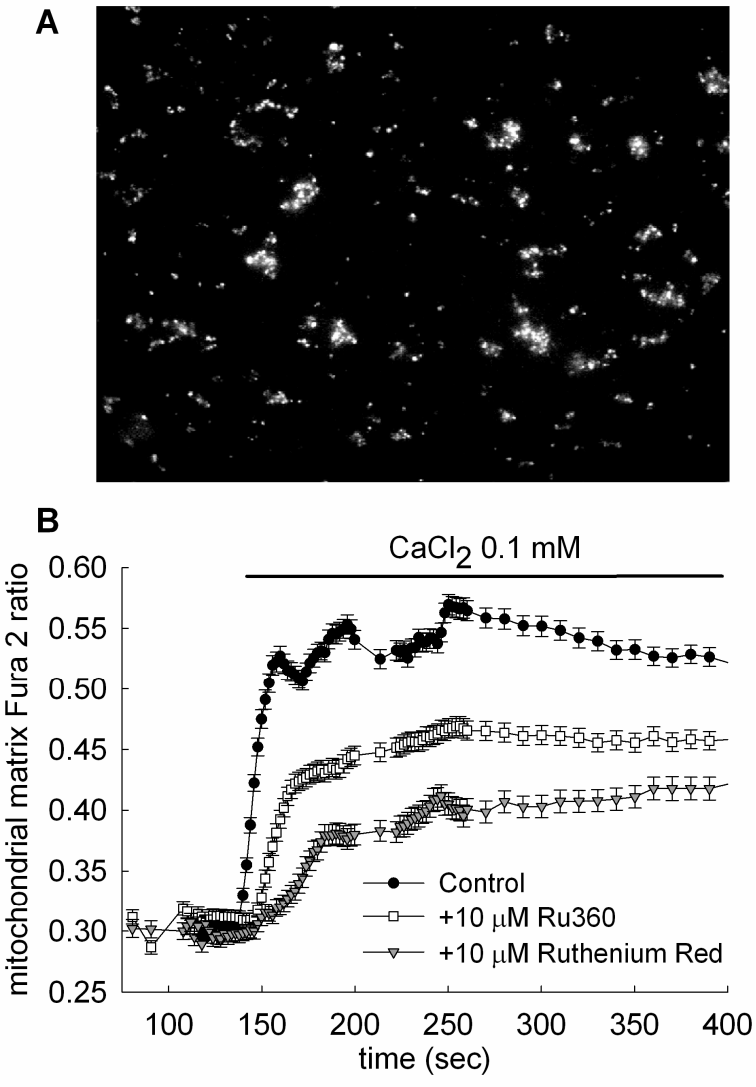

Figure 7. Effect of the Ca^{2+} uniporter inhibitors Ru360 and Ruthenium Red on mitochondrial matrix Ca^{2+} accumulation of isolated WT brain mitochondria imaged under wide-field epifluorescence. A: Wide-field epifluorescence image of isolated brain mitochondria from WT mice, loaded with fura 2 AM. **B**: Time recordings of mitochondrial-trapped fura 2 fluorescence of immobilized mitochondria, perfused by 0.1 mM $CaCl_2$ in the presence of absence of Ca^{2+} uniporter inhibitors as indicated in the panel, in the absence of exogenous substrates. Results are representative of at least 4 independent experiments.

provide further evidence for this, we loaded isolated mitochondria with Fura 2, and imaged them under wide-field epifluorescence (**Figure 7**, *panel A*). This experimental setup benefits from *i)* the spatial resolution in Fura 2 imaging, avoiding a "contaminant" signal of leaked Fura 2 in the extramitochondrial space and *ii)* provides a valid quantitative signal of matrix [Ca^{2+}] in the submicromolar range. Surprisingly, isolated mitochondria perfused with a buffer containing 0.1 mM $CaCl_2$ showed robust increases in matrix-entrapped Fura 2 fluorescence that exhibited only a partial sensitivity to Ru360 (10 µM) and ruthenium red (10 µM), *panel B*, arguing against the assumption that Ca^{2+} was acting exclusively on an extramitochondrial site when inducing changes in light scatter.

4.1.4. Effect of respiratory chain inhibition on Ca^{2+}-induced PTP

To address the contribution of respiratory chain components to the protective effect of substrates on Ca^{2+}-induced changes in light scatter, we pretreated mitochondria with complex I (rotenone or piericidin A), complex III (myxothiazol or stigmatellin), and complex IV (KCN) inhibitors. The emerging picture depicted from **Figure 8** was that rotenone or piericidin A (traces *c*, *d* of *panel A* and traces *b*, *c* of *panel B*) afforded protection from Ca^{2+}-induced changes in light scatter, irrespective of the presence or abscence of substrates, while myxothiazol, stigmatellin and KCN not only falied to confer protection, they also negated the protective effect of substrates (traces *e*, *f* of *panel A* and traces *b*, *c*, *d*, *e*, *f* of *panel C* of **Fig. 8**; see also **Figure 8**, *panel D*). High concentrations of myxothiazol and stigmatellin (10 µM and 2 µM, respectively) that also block complex I [181], failed to afford protection, as opposed to rotenone and piericidin A. However, rotenone and piericidin A (as well as rolliniastatin used in [80]), bind to a different site than myxothiazol and stigmatellin [181]. Maximum swelling rates pooled from all experiments (expressed as in **Figures 5** and **6**) for each condition and after each Ca^{2+} pulse is shown in *panel D*

of **Figure 8**. Inhibition of PTP by rotenone has been previously reported

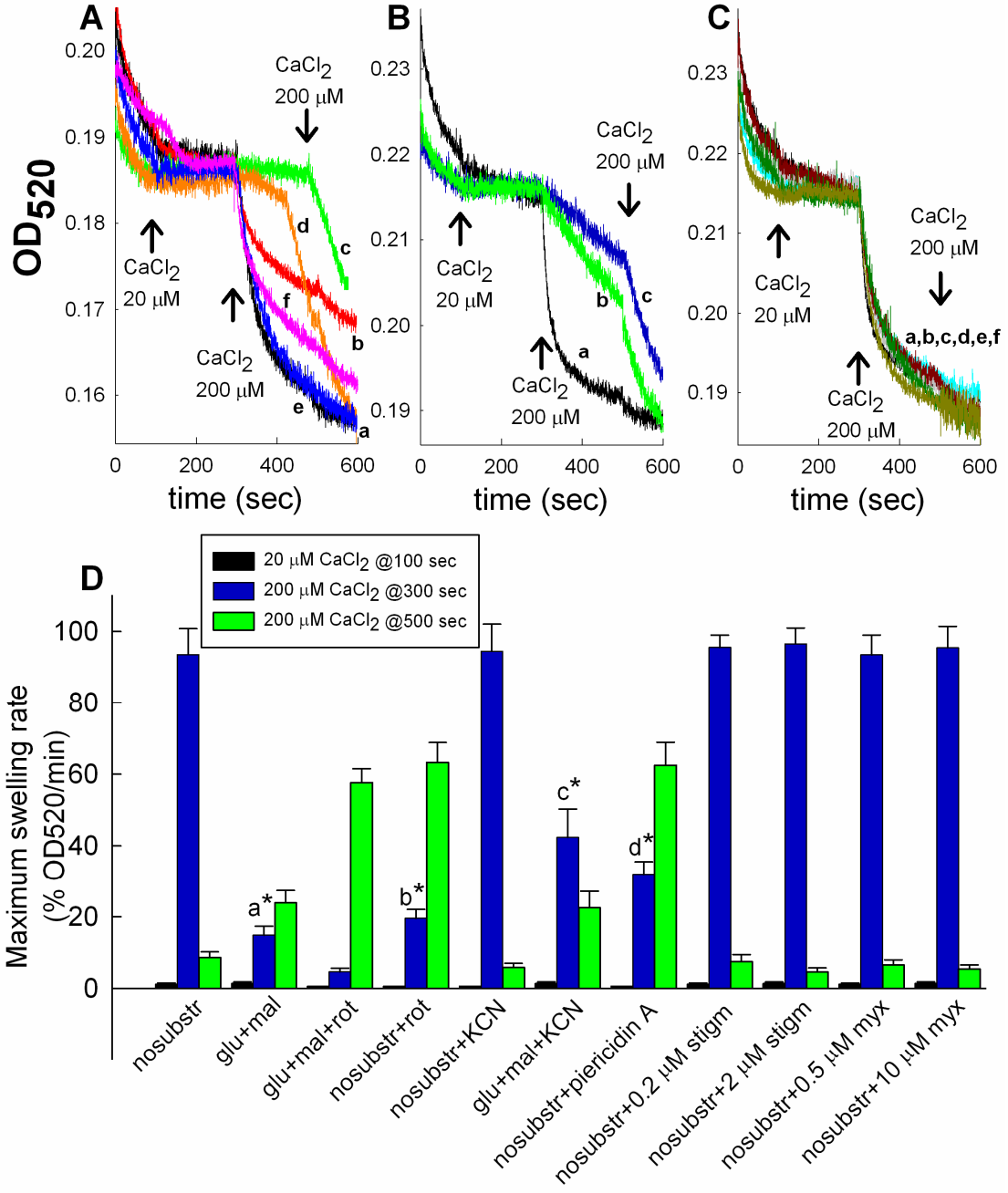

Figure 8. Effect of respiratory chain inhibition on Ca^{2+}-induced PTP. Traces of light scatter recorded spectrophotometrically at 520 nm during $CaCl_2$ additions at the concentrations indicated in the figures, to mitochondrial suspensions. All experiments were performed on WT mice. **A**: *a*: no substrates; *b*: plus glu+mal; *c*: plus glu+mal + 1 µM Rotenone; *d*: no substrates + 1 µM Rotenone; *e*: no substrates + 1 mM KCN; *f*: plus glu+mal + 1 mM KCN. **B**: *a*: no substrates; *b*: no substrates + 1 µM Piericidin A; *c*: no substrates + 1 µM Rotenone. **C**: *a*: no substrates; *b*: no substrates + 0.2 µM stigmatellin; *c*: no substrates + 2 µM stigmatellin; *d*: no substrates + 0.5 µM myxothiazol; *e*: no substrates + 10 µM myxothiazol; *f*: no substrates + 1 mM KCN. Results are representative of at least 4 independent experiments. Panel **D** depicts the maximum swelling rates pooled from all individual experiments (expressed as in **Figures 5** and **6**) for each condition and after each Ca^{2+} pulse. Error bars represent S.E.M.; a is statistically significant from c, $p<0.05$; b is statistically significant from d, <0.05, one-way ANOVA on Ranks.

[73;80;177;182]. Since the protective effect of substrates was negated by cyanide, we decided to use this regimen for testing mitochondrial swelling within neurons and astrocytes, since the *in situ* availability of substrates is much less amenable to manipulation.

Trace	Figure 8, *panel A*	Mitochondrial PTP-inhibitory effect
a	No substrate	∅
b	Glutamate+malate (substrates)	∅
c	Glutamate-malate + 1μM Rotenone	√
d	No substrate + 1μM Rotenone	√
e	No substrate + 1mM KCN	∅
f	Glutamate-malate + 1mM KCN	∅

Trace	Figure 8, *panel C*	Mitochondrial PTP-inhibitory effect
a	No substrate	∅
b	No substrate + 0,2μM Stigmatellin	∅
c	No substrate + 2μM Stigmatellin	∅
d	No substrate + 0,5μM Myxothiazole	∅
e	No substrate + 10μM Myxothiazole	∅
f	No substrate + 1mM KCN	∅

	Figure 8, *panel B*	
a	No substrate	∅
b	No substrate + Piericidin-A 1μM	√
c	No substrate + 1μM Rotenone	√

Table 2. Effect of respiratory chain inhibitors on Ca^{2+}-induced PTP.

On **Table 2**, the effect of complex I, III and IV inhibitors on Ca^{2+}-induced PTP depicted in **Figure 8** is summarized, highlighting the fact that only Rotenone and Piericidin A binding to complex I on a specific binding site are protective, while inhibition of the respiratory chain elsewhere even negates the protective effect of substrates.

4.1.5 Effect of CypD ablation on Ca^{2+}-induced mitochondrial swelling within neurons and astrocytes

To address the role of CypD in the opening of brain-specific PTP *in situ*, swelling of CypD-deficient versus wild type mitochondria within neurons or astrocytes of the same culture were compared during Ca^{2+} overload, induced by addition of calcimycin (1 µM 4Br-A23187). Mitochondria were visualized by wide field epifluorescence imaging of mitochondrially targeted DsRed2. Astrocytes grew as a monolayer on the bottom of the chamber, while neurons grew as a monolayer above them. Cultures were prepared at the same age from the WT and KO mouse pups (P0 or 1) and measurements were performed in the same range of *days in vitro*; accordingly, the neurons/astrocytes ratio deviated minimally from one culture to another (2-2.6), deduced from counting cells from images of fura-loaded cultures. Neurons and astrocytes were distinguished by their different mitochondrial morphology [183]. Neuronal mitochondria are typically more densely packed in the soma, therefore dendritic mitochondria were chosen for analysis. Astrocytes are flatter than neurons in culture, and they exhibited elongated, branched mitochondria of even thickness. Mitochondrial swelling was monitored by evaluating DsRed2-visualized mitochondrial morphology by calculation of changes in mean mitochondrial diameters using the thinness ratio technique. In these assays the onset of swelling was defined by the sudden decrease in the thinness ratio. As shown in **Figure 9 A**, both WT and CypD-KO mitochondria within neurons swelled and fragmented in response to Ca^{2+} overload induced by the addition of calcimycin within 600-800 sec.

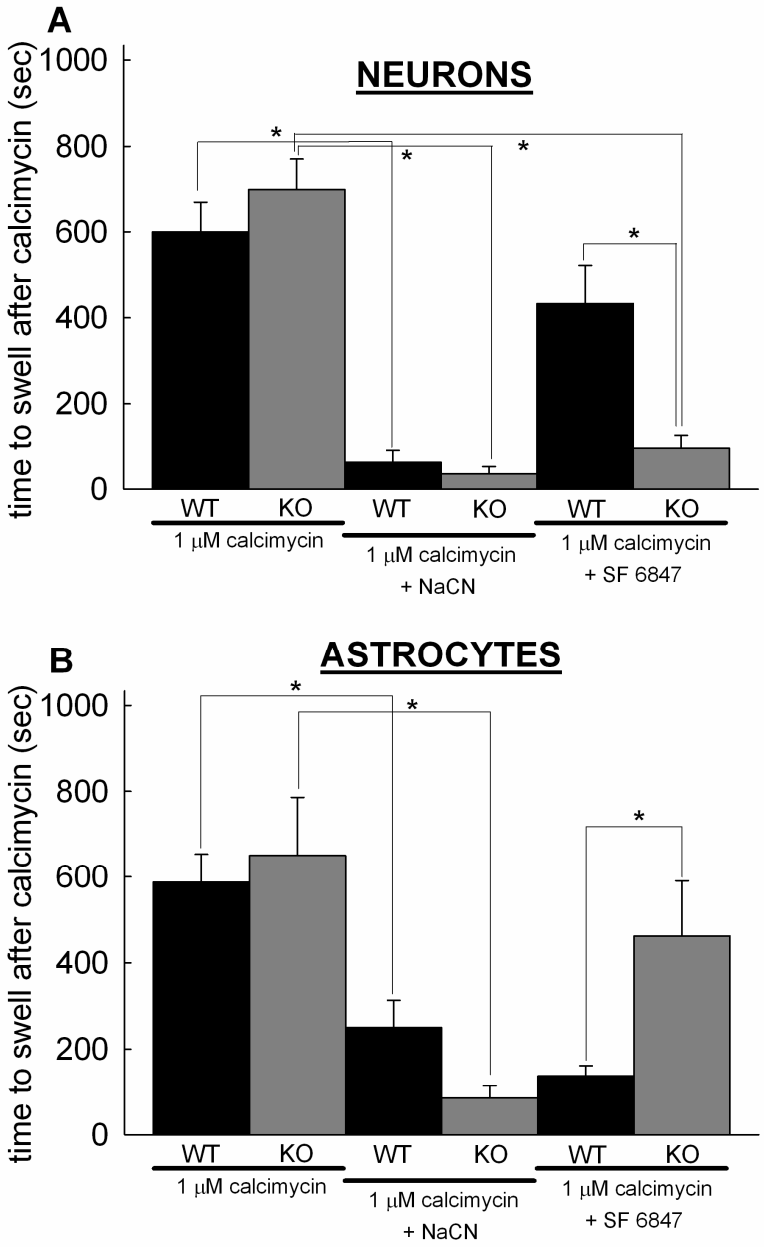

Figure 9. Effect of CypD ablation on Ca^{2+}-induced mitochondrial swelling within neurons and astrocytes. **A-B**: Time elapsed between calcimycin application and mitochondrial swelling was detected by wide field imaging of mito-DsRed2 expressing neurons (**A**) and astrocytes (**B**) in mixed cortical cultures from wild type (black bars) or CypD-KO (gray bars) mice. The onset of swelling was determined by detection of an increase of mean diameter of mitochondria in the microscopic view field by calculation of the thinness ratio. Co-application of 5 mM NaCN and calcimycin was performed in a medium without glucose supplemented with 2 mM 2-deoxyglucose. Bars indicate means ± S.E.M. of 4-12 cells (*, $p<0.05$ significance by Kruskal-Wallis ANOVA on Ranks).

When NaCN was co-applied with calcimycin in a glucose-free media in the presence of 2 mM 2-deoxyglucose, swelling of mitochondria was almost immediate in both wild type and CypD-KO neurons. However, Ca^{2+} overload of uncoupled mitochondria (by co-application of 1 µM SF 6847) triggered swelling at a significantly earlier time in CypD-KO than in wild type neurons. In contrast to the neurons, Ca^{2+} overload of uncoupled mitochondria triggered swelling at a significantly earlier time in wild type than in CypD-KO astrocytes (**Figure 9 B**). In the absence of glucose and concomitant presence of 2-deoxyglucose and NaCN, in situ mitochondria are almost certainly completely depolarized. We used calcimycin at 1 µM concentration that likely affects only the Ca^{2+}-permeability of the plasma membrane. Experiments on cultured neurons and astrocytes loaded with fura 2 (K_d=225 nM, [184]) versus fura 6F (K_d=2.47 µM, [170]) revealed that the increase in cytosolic Ca^{2+} by 1 µM calcimycin was in the 1-2 µM range in contrast to the 1.3 mM in the medium (not shown); thus the amount of calcimycin distributed in the plasma membrane was very small and unlikely for it to distribute in the inner mitochondrial membrane.

4.1.6. Effect of CypD ablation on in situ mitochondrial swelling of neurons challenged by glutamate

In order to expose neuronal in situ mitochondria to high-Ca^{2+} challenge by an alternative mechanism, neurons were exposed to excitotoxic levels of glutamate and glycine, in the absence of Mg^{2+}. Mitochondrial swelling was monitored by thinness ratio values calculated from wide field fluorescence images of mitochondrially targeted DsRed2. Glutamate exposure triggered a biphasic mitochondrial swelling response (shown for a WT neuron) indicated by the decrease of the thinness ratio (**Figure 10 A**, black circles). Swelling comprised of an initial, 1^{st} and a well separated, delayed 2^{nd} drop. The 1^{st} drop of thinness ratio invariably coincided with the initial $[Ca^{2+}]_i$-response to glutamate and the 2^{nd} drop to the secondary, irreversible rise of $[Ca^{2+}]_i$, termed delayed calcium deregulation, DCD [185-187] (**Figure 10 A** and **B**, black bars). In cultures prepared from CypD-KO mice (**Figure 10 B**, gray bars) the first phase of mitochondrial swelling was detected only in 60% of the neurons. Furthermore, only 40 % of CypD-KO neurons exhibited the secondary swelling of mitochondria during DCD (**Fig. 10 B**). Finally, the initial swelling of mitochondria was significantly delayed in CypD-KO neurons compared to wild type, while the time of onset of the secondary mitochondrial swelling was not statistically different (**Figure 10 C**).

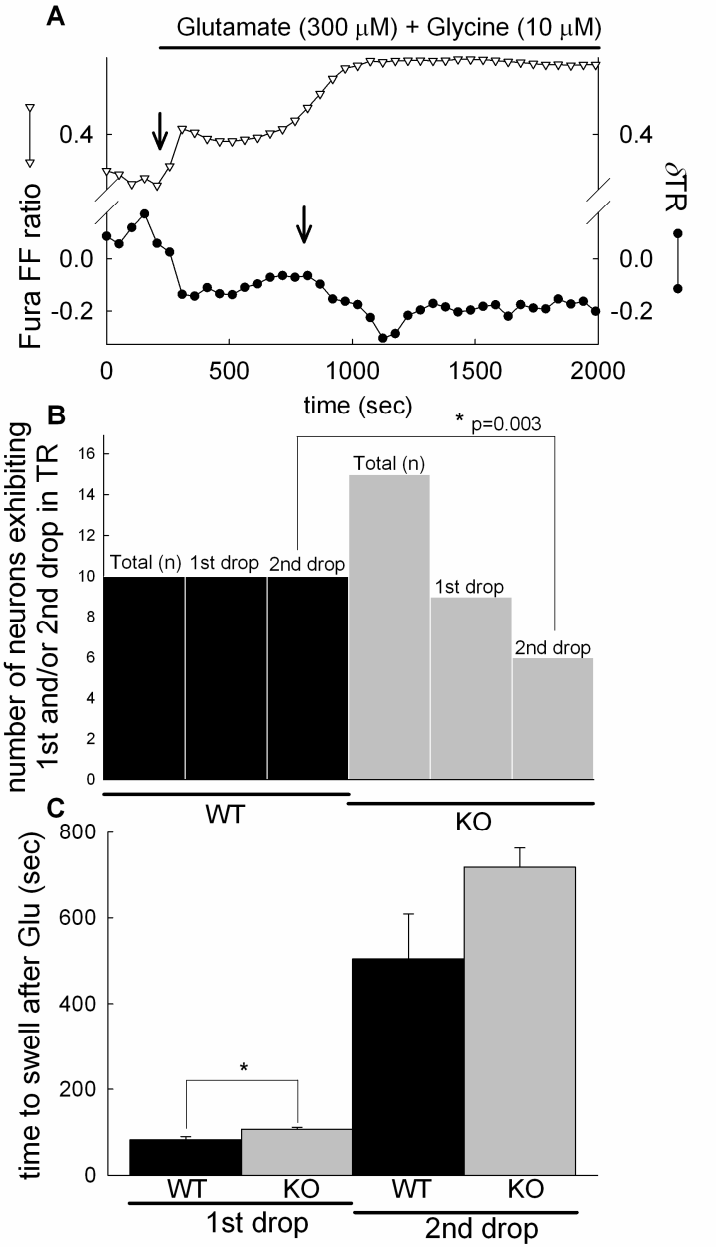

Figure 10. Effect of CypD ablation on glutamate-evoked biphasic mitochondrial swelling in cortical neurons. **A**: Wide field fluorescence time lapse recording in Fura-FF-AM loaded wild type cortical neuron expressing mito-DsRed. Glutamate (300 μM) plus glycine (10 μM) in the absence of $[Mg^{2+}]_e$ evoked a rise of $[Ca^{2+}]_i$ indicated by the increasing ratio of Fura-FF 340/380nm fluorescence intensities (triangles). Mitochondrial swelling was measured by calculating thinness ratio (TR) of mito-DsRed fluorescence images (circles), where swelling is marked by the decreasing thinness ratio (arrows). The 1st and 2nd drops of the thinness ratio always coincided with the initial response to glutamate and to the DCD, respectively. Representative traces of 10 recordings.
B: Quantification of the observation of 1st and 2nd drops in neurons from wild type (black bars) and CypD-KO mice (grey bars) using Fisher exact test. Total (n) corresponds to the number of cells observed and 1st and 2nd drops to the observation of the drops in the thinness ratio in recordings similar to (**A**). **C**: The onset of mitochondrial swelling was defined as the time elapsed between the application of glutamate and the sudden decrease of the thinness ratio, bars show mean ± S.E.M. 10 cells (*, $p<0.05$ significance by Kruskal-Wallis ANOVA on Ranks).

4.1.7. Discussion

There are hundreds of publications addressing permeability transition with relation to various aspects of bioenergetics; hereby we attempted to shed light on the phenomenon where CypD-dependent PTP precedes necrotic events during which there is energy crisis, but not apoptosis, a mechanism that is dependent on energy provision. We have narrowed our investigations to brain mitochondria in isolation, and within their natural environment (both neurons and astrocytes).

The most important finding of this study is the dramatic hastening of the swelling of in situ neuronal and astrocytic mitochondria by glucose deprivation and NaCN co-application, upon calcimycin exposure. This extends the previous findings on isolated mitochondria [81;185;188-191] and the results of this study, showing that a diminished electrochemical gradient primes mitochondria within their natural environment to undergo Ca^{2+}-induced PTP. We created depolarizing conditions by three different means: *i)* substrate deprivation (no electron flow), *ii)* ETC inhibitors (no electron flow), and *iii)* presence of an uncoupler (high electron flow). Results were not entirely congruent between isolated versus *in situ* mitochondria (i.e. compare presence versus absence of substrates or uncoupler), but in both experimental models the presence of cyanide prompted pore opening. Our findings support the notion that the lack of an electrochemical gradient unfavoring electrophoretic Ca^{2+} uptake not only fails to protect *in situ* mitochondria from PTP, but it also subserves the purpose of decreasing a threshold to the point that either an increase in matrix Ca^{2+} concentration due to a mere diffusion and/or an extramitochondrial site with low affinity for Ca^{2+}, induces pore opening. However, our findings are partially at odds with those obtained in [192], in which the effect of cyanide was found to disfavor PTP opening. The difference may stem from the fact that in that study isolated skeletal muscle mitochondria were investigated.

The swelling induced by high-Ca^{2+} in energized in situ neuronal and astrocytic mitochondria was not CypD-dependent. To this we must stress that our results on isolated mitochondria point to the possibility of an Ru360/Ruthenium-Red-insensitive route for Ca^{2+} entry. Furthermore, our results also show that there are cell-specific differences of the same tissue regarding the bioenergetic contribution to Ca^{2+}-induced PTP. For example, it is striking that the elapsed time upon calcimycin exposure until the onset of swelling of uncoupler-treated neuronal WT mitochondria was smaller than that recorded for CypD-KO mitochondria, and the exact opposite was observed in astrocytes.

There are ~1500 proteins in mitochondria and less than 3% of those are mitochondrially encoded [193], while the rest are nuclear-encoded. It is at least prudent to consider that the composition and/or regulation of the mitochondrial permeability transition pore exhibits tissue or even cell-specific differences, as it has been suggested elsewhere [194;195].

4.2. Ca^{2+} release triggered by NAADP in hepatocyte microsomes

4.2.1. NAADP induces Ca^{2+} release from hepatocyte microsomes

Hepatic microsomal vesicles rapidly sequestered $^{45}Ca^{2+}$ in the presence of ATP (**Figure 11 A**), with an uptake of 4.0 ± 0.2 nmol/mg protein (n=13). The maximum of Ca^{2+} uptake was found within 5-10 minutes, which is slower than that observed in experiments with intact or permeabilized cells but consistent with earlier reports [196]. About 90% of the specifically retained microsomal Ca^{2+} was rapidly released by ionomycin (5 µM) (**Figure 11 A**). This rate of decline of microsomal Ca^{2+} content defined the magnitude of the microsomal Ca^{2+} stores available for release. We found it important to identify of the main Ca^{2+} transporter through which the microsomes are loaded. We determined the Ca^{2+} uptake of liver microsomes in the presence of 1 µM thapsigargin, a selective inhibitor of the sarco(endo)plasmic reticulum Ca^{2+}-ATPase (SERCA) and 1 µM bafilomycin A1, an established blocker of the V-type ATP-ase [197]. The Ca^{2+} accumulation of microsomes was nearly abolished by thapsigargin, while bafilomycin does not affect substantially the Ca^{2+} uptake mechanisms of liver microsomes. In the light of these results, it is the SERCA that represents the main mechanism responsible for the active loading of liver microsomes. In the next step, we investigated whether NAADP could induce Ca^{2+} release from rat liver microsomes loaded actively with $^{45}Ca^{2+}$ and compared it to $InsP_3$ and cADPR-induced Ca^{2+} release. In this assay, NAADP (10 µM), $InsP_3$ (10 µM) and cADPR (10 µM) induced a fast Ca^{2+} efflux, which differed significantly from control microsomes (CICR) (**Figure 11 B**). The pattern of NAADP mediated Ca^{2+} release appeared to be biphasic, with an initial rapid release followed by a sustained but slower phase of

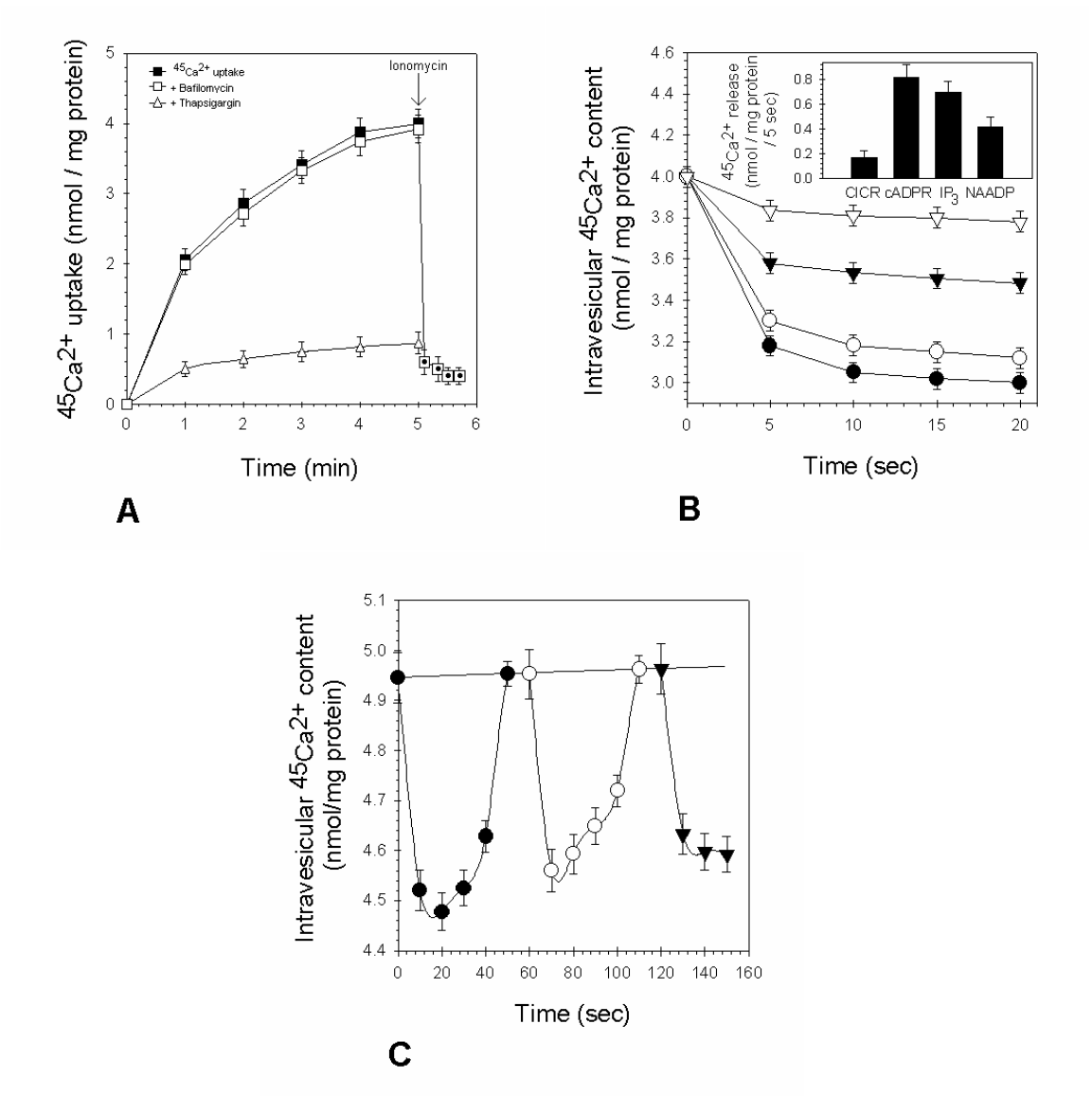

Figure 11. NAADP-induced $^{45}Ca^{2+}$ release from active loaded hepatocyte microsomes. (**A**) The time course of the Ca^{2+} uptake by liver microsomes was determined using $^{45}Ca^{2+}$, as described in the 'Materials and Methods' section **(Section 3.7)**. Accumulation (■) of Ca^{2+} was started by addition of 1 mM ATP. The amount of the mobilizable Ca^{2+} was determined by adding 5 µM ionomycin (⊡) to the medium. The effect on $^{45}Ca^{2+}$ uptake of 1 µM thapsigargin (Δ) and 1 µM bafilomycin (□) was also tested. Bafilomycin was added to the microsomes 5 minutes before $^{45}Ca^{2+}$ uptake was initiated.
(**B**) Comparison of the Ca^{2+} mobilizing characteristics of $InsP_3$ (○), cADPR (●) and NAADP (▲) (10 µM each). Ca^{2+}-induced Ca^{2+} release (CICR) (Δ) was determined by adjusting extravesicular free Ca^{2+} level to pCa=6 using EGTA (100 µM). Results are the average ± s.e.m. of 6-12 determination on at least four different experimental days. The inset shows the total amount of Ca^{2+} efflux triggered by $InsP_3$, cADPR and NAADP after 5 seconds of Ca^{2+} release.
(**C**) Microsomes sequestered Ca^{2+} in the presence of an ATP regenerating system (2 U/ml creatine-kinase, 4 mM phosphocreatine) and released calcium in response to subsequent addition of 10 µM cADPR (●),10 µM $InsP_3$ (○) and 10 µM NAADP (▲).

release. A similar pattern of Ca^{2+} release was observed when cADPR and $InsP_3$ were added (**Figure 11 B**). After 5 seconds of Ca^{2+} release the total

amount of Ca^{2+} efflux elicited by CICR was 0.165 ± 0.06 nmol/mg protein (4.6% of ionomycin release, n=6-12). In the same set of experiments, NAADP released 0.42 ± 0.08 nmol Ca^{2+}/mg protein (11.8% of ionomycin release, n=15), while cADPR elicited 0.821 ± 0.1 nmol Ca^{2+}/mg protein (22.8% of ionomycin release, n=10) (**Figure 11 B**, *inset*). Under the same conditions, $InsP_3$ released 0.7 ± 0.09 nmol Ca^{2+}/mg protein (19.6% of ionomycin release, n=8) (**Figure 11 B**, *inset*). Thus NAADP is a potent, but somewhat less effective Ca^{2+} releasing messenger than cADPR and $InsP_3$ in liver hepatocyte microsomes.

To further determine whether the NAADP-induced Ca^{2+} release mechanism in liver microsomes is distinct from the $InsP_3$- and cADPR-mediated Ca^{2+} release mechanism, we tested for possible agonist cross-desensitization. As shown in **Figure 11 C**, we tested subsequent Ca^{2+} release from actively loaded liver microsomes by cADPR, $InsP_3$ and NAADP (all applied at supramaximal concentrations, 10 µM) in the presence of an ATP-regenerating system. NAADP managed to elicit maximal Ca^{2+} efflux when applied after cADPR and $InsP_3$ have already been probed. Thus cross-desensitization to $InsP_3$ and cADPR by NAADP did not occur (**Figure 11 C**). This result further supports the view that NAADP acts upon a Ca^{2+} release mechanism distinct from that of $InsP_3$ and cADPR from rat liver microsomes.

4.2.2. Dose-dependence of the NAADP-mediated Ca^{2+} release

NAADP induced Ca^{2+} release in rat liver microsomes in a dose-dependent manner, with a half-maximal concentration (EC_{50}) of 0.93 ± 0.1 µM (**Figure 12**). Our results correspond with those of other authors who experimented with microsomes prepared from other mammalian tissues [117;118;121], whereas the EC_{50} for NAADP was reported to be one order of magnitude smaller in intact cells (in the range of 100 nM) [113;120].

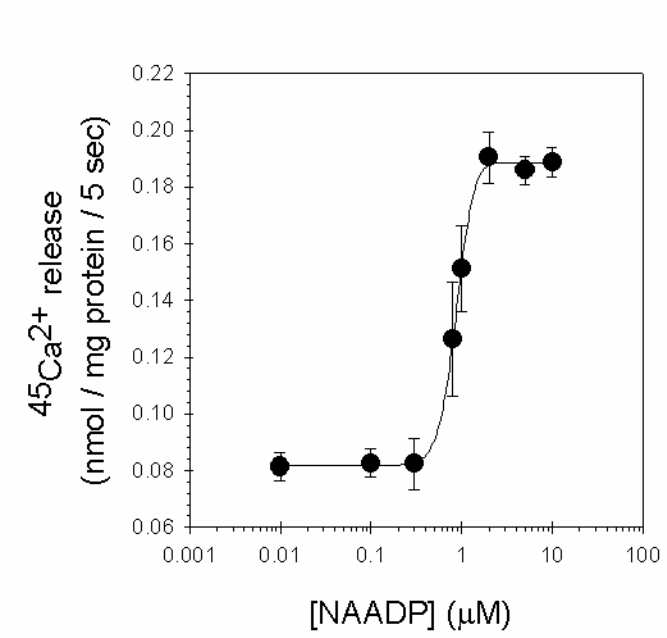

Figure 12. Dose dependence of the NAADP-induced Ca^{2+} release in rat liver microsomes.

Experimental settings were similar to those shown in **Figure 11 B** and the data are representative for five independent experiments.

4.2.3. Unique homologous desensitization pattern of the NAADP receptors

We investigated the inactivation phenomenon of NAADP-induced Ca^{2+} release in liver microsomes. First injection of subthreshold concentration of NAADP (0.1 µM) to microsomes at the third minute during active loading did not result in substantial Ca^{2+} release by itself (**Figure 13 A**). However after 2 minutes of incubation, 10 µM NAADP released 0.14 ± 0.04 nmol Ca^{2+}/mg protein compared to 0.39 ± 0.04 nmol/mg protein Ca^{2+} released from non pre-incubated microsomes.

On **Figure 13 B** we compared the dose-response curve of the NAADP-induced Ca^{2+} release with the curve for residual Ca^{2+} release by supramaximal NAADP (10 µM) after 2 minutes pre-incubation of microsomes with different concentrations of NAADP (between 0.1 nM

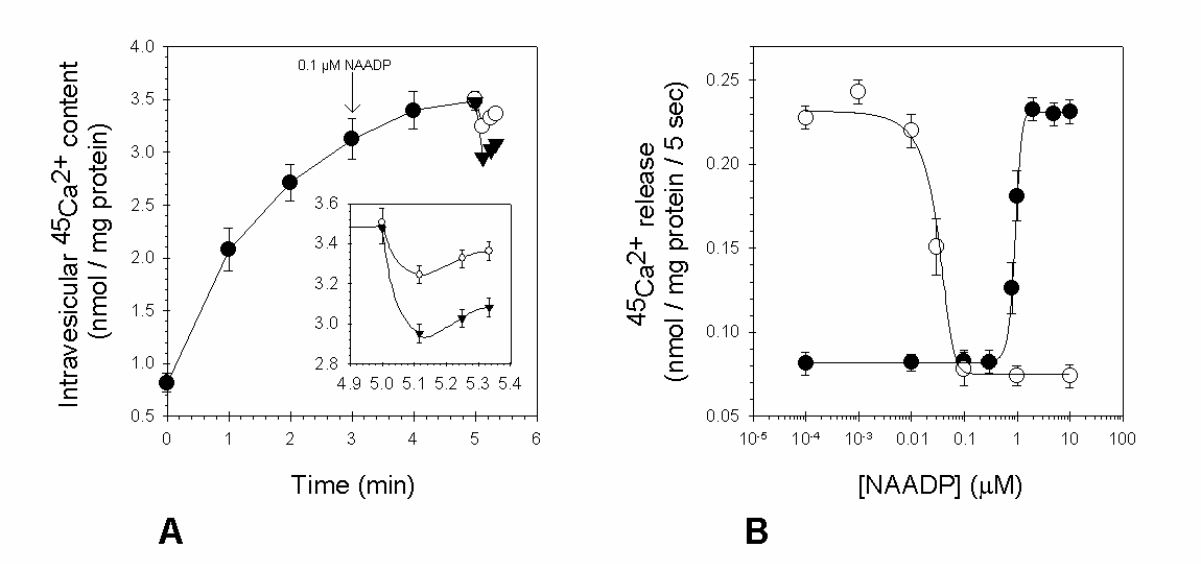

Figure 13. Unique homologous desensitization pattern of the NAADP receptors.
(**A**) Homologous desensitization of NAADP receptors by subthreshold concentrations of NAADP. Actively loaded microsomes (●) were pre-treated with 0.1 µM NAADP for two minutes and then challenged to a supramaximal concentration of 10 µM NAADP (○). NAADP induced Ca^{2+} release from non pre-treated microsomes (▲). The inset shows the Ca^{2+} efflux at five minutes of Ca^{2+} loading from microsomes incubated by non-activating concentration of NAADP and non pre-treated microsomes.
(**B**) Dose-response curve of NAADP (●) and the residual Ca^{2+} release by supramaximal concentration of NAADP (10 µM) after 2 min preincubation with concentrations of NAADP between 0.1 nM and 10 µM (○).

and 10 µM). In this manner, NAADP may function as its own specific antagonist with an IC_{50} of 30 nM. The two curves form a U-shape as NAADP desensitize its receptors with an IC_{50} that is one order of magnitude lower than the EC_{50}. Thus, we found evidence that, similarly to invertebrates [130], full desensitization of the NAADP receptors by subthreshold NAADP concentrations is possible without any need for previous substantial Ca^{2+} release. This phenomenon is in contrast to the self-desensitization mechanism for $InsP_3$ and cADPR (X-desensitization) [130].

4.2.4. The effect of thapsigargin and bafilomycin A1 on the NAADP-evoked Ca^{2+} release in rat liver microsomes

The NAADP sensitive Ca^{2+} stores are insensitive to thapsigargin in sea urchin eggs [198] as well as in several intact mammalian cell types (e.g. arterial smooth muscle [147] and pancreatic acinar cells [141]), and can be localised in the lysosomal compartment [139;147] (acidic thapsigargin-insensitive pool). Therefore, it seemed important to test whether the NAADP-mediated Ca^{2+} release from rat liver microsomes is dependent on acidic pools. One way of interfering with organellar acidfication is to pretreat with bafilomycin A1, which is a blocker of the vacuolar type H^+-ATPase [197]. When actively loaded microsomes were incubated for at least 5 minutes with bafilomycin A1 (1 µM), we found that both NAADP (10 µM) and cADPR (10 µM) elicited an entirely normal Ca^{2+} release response (**Figure 14**; n=4). No substantial change was observed in the response of the Ca^{2+} release elicited by cADPR and NAADP to bafilomycin when longer incubation time (10 and 20 minutes) was applied (unpublished data). These data indicate that the Ca^{2+} release from liver microsomes induced by NAADP in unlikely to come from acidic compartments.

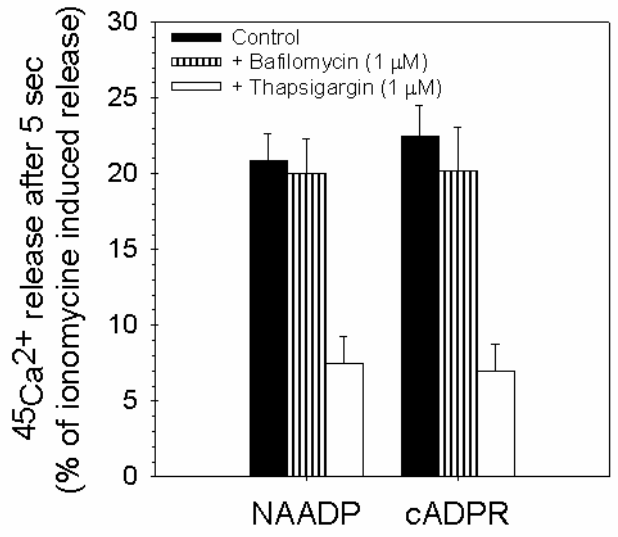

Figure 14. The effect of thapsigargin and bafilomycin A1 on the cADPR- and NAADP-elicited Ca^{2+} release in rat liver microsomes.
The actively loaded vesicules were pre-incubated by thapsigargin (1 µM) for at least 2 minutes and by bafilomycin A1 (1 µM) for at least 5 minutes before Ca^{2+} release was induced with supramaximal concentrations of cADPR and NAADP (both 10 µM). Filled bars represent the Ca^{2+} release from non pre-treated microsomes while open bars show the Ca^{2+} efflux from microsomes treated with thapsigargin (1 µM) and dashed bars represent the effect of bafilomycin A1 (1 µM).

Furthermore, microsomes were treated with maximal concentration of thapsigargin (1 µM), a potent and selective inhibitor of the SERCA, for at least 2 minutes when Ca^{2+} uptake reached the plateau. The amount of Ca^{2+} efflux elicited by 10 µM NAADP in liver microsomes pre-treated with thapsigargin was reduced to 7.48 ± 1.75% of the ionomycin release, while NAADP released 20.86 ± 1.8% of ionomycin release in non pre-treated microsomes (**Figure 14**). The effect of cADPR was similarly affected by pre-treatment with thapsigargin (6.94 ± 1.85% of ionomycin release in pre-incubated microsomes compared to 22.51 ± 2% of ionomycin release in the absence of thapsigargin). Our results show that the NAADP mediated Ca^{2+} release was thapsigargin dependent as well as that of cADPR. The ability of thapsigargin to block the NAADP-sensitive Ca^{2+} release is in contrast to the results published for sea urchin eggs [198] or intact mammalian cells [141;147]. The Ca^{2+} release from microsomes can be described as a one-pool model [111]. The

microsomal Ca^{2+} store is in fact a mixture of Ca^{2+} stores deriving from both lysosomes and the ER, moreover it is filled mainly by SERCA (see **Fig. 14 A**) and contains $InsP_3Rs$, RyRs and NAADPRs. This type of fusion of the different intracellular Ca^{2+} stores is an artefact as to the result of the preparation process itself.

4.2.5. Ca^{2+} and pH dependence of the NAADP-induced Ca^{2+} release

In the next set of experiments, we investigated the effect of free extravesicular Ca^{2+} concentration upon the Ca^{2+}-release induced by NAADP, $InsP_3$ and cADPR (**Figure 15 A**). Passive loading of microsomes (described in **Section 3.8.**) has the advantage over ATP-driven loading that the concentration of free extravesicular Ca^{2+} can be set more accurately with Ca^{2+} complexing agents, such as EGTA. The activation of both $InsP_3$ receptors and RyRs often shows similar bell-shaped dependence on the concentration in the vicinity of the cytoplasmic face of the release [199;200]. Similarly, in **Figure 15 A** we show that the pCa response curves of the $InsP_3$ and cADPR appeared to be bell-shaped with an optimal pCa at 7 and 6 respectively. However, the NAADP-induced Ca^{2+} release we found to be fairly independent of the extravesicular Ca^{2+} concentration. This finding is one of the unique characteristics that NAADP displays in all cell types.

It was described previously that the NAADP-induced calcium release in sea urchin egg homogenates [201] and rat mesangial cell microsomes [122] was not affected by the pH changes of the incubation medium. In contrast, cADPR-induced Ca^{2+} release was inhibited by alkalinization of the media [201]. We found that the NAADP-induced Ca^{2+} release in hepatocyte microsomes was not affected by changing the pH of the incubation buffer from 6.4 to 7.8 (**Figure 15 B**). We propose that protonation and deprotonation of relevant amino acids with pK values in the range of physiological pH has no effect upon the gating

property of the putative channel that is activated by NAADP and, by extension, upon the binding of NAADP to its receptor [128]. However, the response to cADPR was mostly dependent on pH, showing an optimal pH of 7.2. The peak Ca^{2+} efflux evoked by cADPR was at least 50%

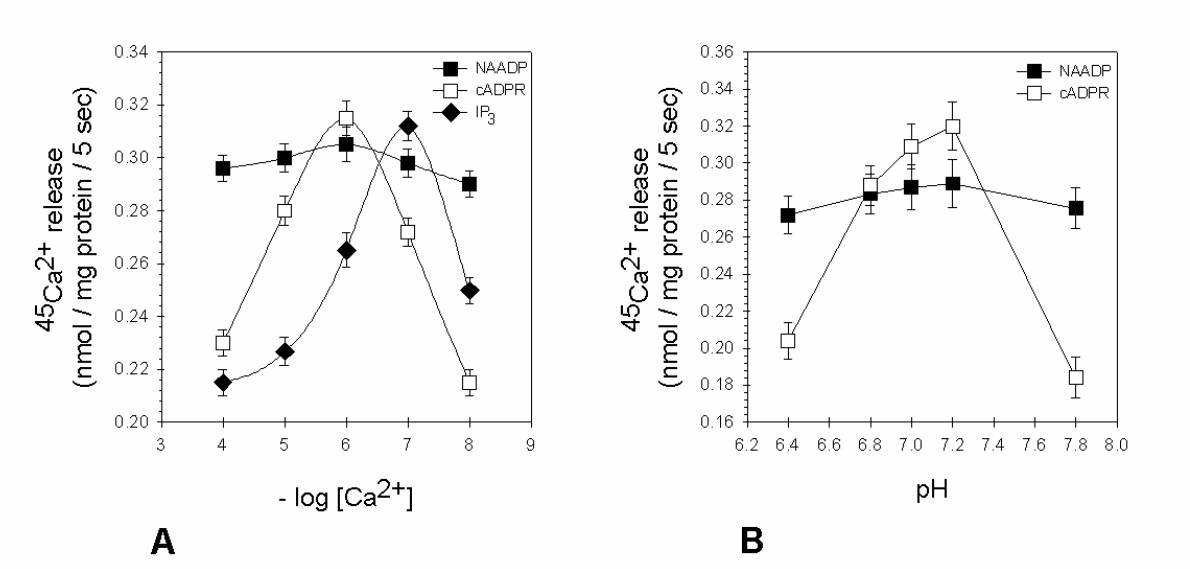

Figure 15. Ca^{2+} and pH dependence of the NAADP-induced Ca^{2+} release.
(**A**) Extravesicular free Ca^{2+} concentration dependence of the $InsP_3$, cADPR and NAADP mediated system in passively loaded liver microsomes. Extravesicular pCa (4-8) was set by EGTA (200-750 µM respectively), NAADP (■), $InsP_3$ (◆) and cADPR (□) were applied in supramaximal concentrations (10 µM).
(**B**) Differential effect of pH on the cADPR and NAADP sensitive Ca^{2+} releasing system. The pH of the Ca^{2+} release medium was changed in a range from 6.4 to 7.8 and the amount of $^{45}Ca^{2+}$ released by 10 µM cADPR (□) and 10 µM NAADP (■) was determined.

higher than at pH values one unit lower or higher. Alkalinization of the media may alter the binding of cADPR to its receptor or may affect activation of RyRs by pharmacological agonists [201]. NAADP- and cADPR-triggered Ca^{2+} release from liver microsomes was differentially affected by pH, providing further evidence that these agonists signal through functionally distinct pathways.

4.2.6. Pharmacological properties of the NAADP-elicited Ca^{2+} efflux

We examined the pharmacological properties of the NAADP mediated Ca^{2+} release to gather more evidence that it is distinct from those mediated by $InsP_3$ and cADPR. Heparin (100 µg/ml), a well-established inhibitor of the $InsP_3R$-s [202], inhibited the Ca^{2+} release elicited by $InsP_3$ by 62.15 ± 7% and did not alter the effect of cADPR

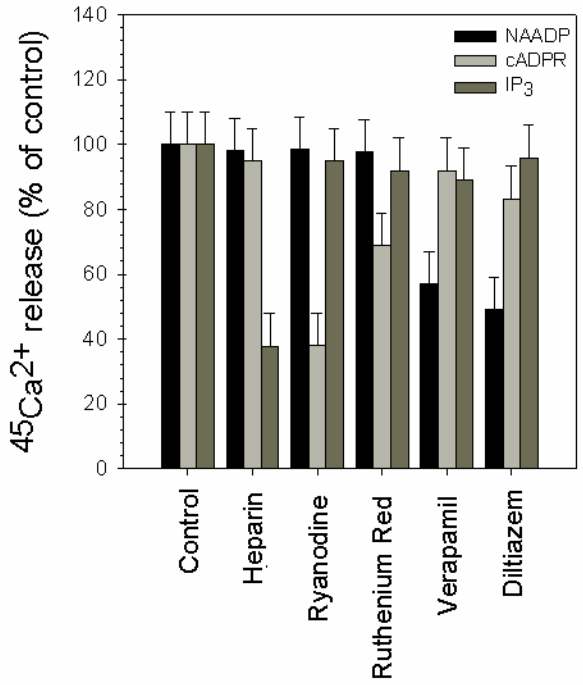

Figure 16. Pharmacological properties of the intracellular Ca^{2+} channels mediated by $InsP_3$, cADPR and NAADP.
The $^{45}Ca^{2+}$ release by supramaximal concentrations $InsP_3$, cADPR and NAADP (all 10 µM) was challenged in the presence of heparin (100 µg/ml), ryanodin (5 µM), ruthenium red (5 µM), verapamil (100 µM) and diltiazem (100 µM).

and NAADP (**Figure 16**). The RyR antagonists, ryanodine (5 µM) and ruthenium red (5 µM), blocked the cADPR-induced Ca^{2+} efflux by 62 ± 6% and 31.19 ± 4% respectively, leaving that of $InsP_3$ and NAADP unaltered. The L-type Ca^{2+} receptor blockers, verapamil (100 µM) and diltiazem (100 µM) [130], abolished specifically, but only partially (up

to 43 ± 4% and 50.82 ± 6% of inhibition respectively) the Ca^{2+} releasing effect of NAADP in rat liver microsomes. On the other hand, they had minimal effect on the Ca^{2+} release by $InsP_3$ and cADPR (less than 15%) (**Figure 16**). To sum up, neither heparin, nor ryanodine and ruthenium red were able to block substantially the NAADP-induced Ca^{2+} release, while verapamil and diltiazem were effective inhibitors of NAADP receptors (**Figure 16**).

	IP_3	cADPR	NAADP
Heparin (100 µg/ml)	62.15 ± 7%	n.s.	n.s.
Ryanodine (5 µM)	n.s.	62 ± 6%	n.s.
Ruthenium red (5 µM)	~ 8%	31.19 ± 4%	n.s.
Verapamil (100 µM)	~ 10%	~ 8%	43 ± 4%
Diltiazem (100 µM)	~ 5%	~ 15%	50.82 ± 6%

Table 3. Inhibition of the Ca^{2+} channels mediated by $InsP_3$, cADPR and NAADP by established blockers of $InsP_3$Rs, RyRs and NAADPRs.
Data are presented as percentage of the reduction of the $^{45}Ca^{2+}$-releasing ability induced by supramaximal concentrations of each messenger.
n.s. stands for inhibition of less than 5%.

On **Table 3**, the inhibitory effect of the forementioned blockers of $InsP_3$Rs, RyRs and NAADPRs are summarized for the sake of clarity, based on the results shown on **Figure 16.**

4.2.7. Discussion

In **Section 4.2.**, we provided evidence, that NAADP is indeed present and functional in hepatocyte microsomes. In the first step, we defined the type of Ca^{2+} store that operates within microsomes based on the thapsigargin sensitivity and bafilomycin A1 insensitivity of both

Ca^{2+} uptake into (**Figure 11 A**) and Ca^{2+} release from microsomes (**Figure 11**). The main pathway for microsomal Ca^{2+} sequestration is through SERCA, since it is abolished by thapsigargin, but left unaltered by bafilomycin A1 (**Figure 11 A**). Also, the one-pool model for Ca^{2+} release is applicable for Ca^{2+} efflux from the microsomal stores, because both the cADPR- and NAADP-mediated Ca^{2+} release are hindered by thapsigargin, but not bafilomycin A1 (**Figure 14**). Thus, unlike in intact cells, cADPR and NAADP mobilize Ca^{2+} from the same, non-acidic pool. Our model for the hepatocyte microsomal Ca^{2+} store is depicted above in **Figure 17**.

Next, we analized several properties of the NAADP-mediated Ca^{2+} release system, which showed a sigmoideal dose-dependence curve with an EC_{50} of 0.93 ± 0.1 µM (**Figure 12**). However, desensitization of receptors for NAADP occurred even when subthreshold concentrations of NAADP were used for pre-incubation (**Figure 13 A**), thus NAADP acts as it's own antagonist with an IC_{50} of ~30nM (**Figure 13 B**). This type of homologue desensitization (U-desensitization) is characteristic for NAADP and has been verified for the first time in a vertebrate tissue by our workgroup. Furthermore, NAADP provides a Ca^{2+}-independent

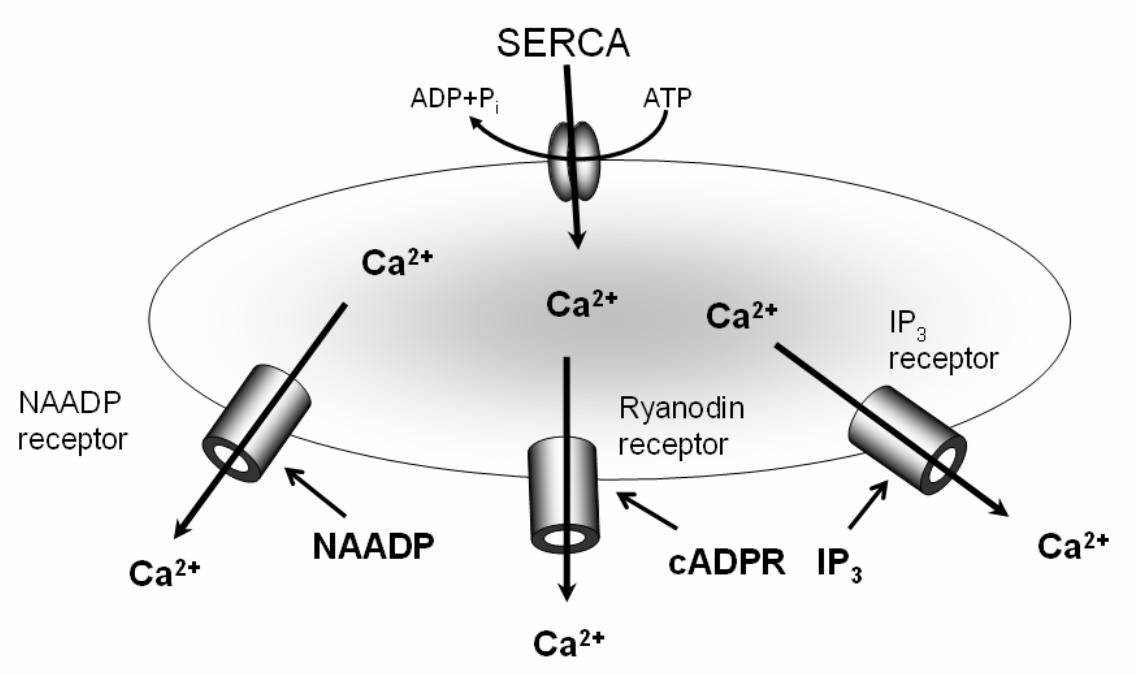

Figure 17. Model for the hepatocyte microsomal Ca^{2+}-store.

(**Figure 15 A**) and non pH-dependent (**Figure 15 B**) system for Ca^{2+} release in hepatocyte microsomes.

Finally, based on the distinct pharmacological properties of the NAADP-induced events (**Figure 16** and **Table 3**), as well as the lack of cross desensitization between $InsP_3$, cADPR and NAADP (**Figure 11 C**), our results altogether suggest that the NAADP-mediated Ca^{2+} release is indeed a distinct pathway in rat liver microsomes.

5. Conclusions

In the past years, I have contributed to the experimental work of the Neurobiochemistry Research Division of the Departement of Medical Biochemistry on Semmelweis University. I participated in the establishment of a novel method for the measurement of the ADP/ATP exchange rate based on the differential affinity of ADP and ATP to Mg^{2+} [53], and the re-evalutaion of the role of matrix acidification in uncoupler-induced Ca^{2+} release from mitochondria [51]. These data have already been presented elsewhere, as well as the results concerning the forward operation of the adenine nucleotide translocase during F_0F_1-ATPase reversal [203].

The present thesis evolves around the brain-specific contribution of CypD to Ca^{2+}-induced PTP and the NAADP-induced microsomal Ca^{2+} release in hepatocytes [116;168].

In **Section 4.1**, we verified that substrate-starved mitochondria are more sensitive to Ca^{2+}-induced PTP than mitochondria supplied with substrates. This effect is CysA sensitive and can be overrided by an excessive Ca^{2+} stimulus (**Figure 5 A** and **B**). Also, substrate-starved mitochondria prepared from CypD KO mice showed similar sensitivity to Ca^{2+}-induced PTP as WT mitochondria exposed to CysA (**Figure 5 D** and **E**). Substrate-starved mitochondria were shown to exhibit PTP in response to high Ca^{2+} additions, despite of the fact that no Ca^{2+} uptake was measured (**Figure 5 F**). Moreover, the inhibition of the major Ca^{2+} uptake routes of WT and CypD KO mitochondria by Ru360 or RuRed did not affect their responses to high-Ca^{2+} (**Figure 6 A** and **B**), raising the possibilities that Ca^{2+} was either inducing CypD sensitive swelling by acting on an extramitochondrial site, or Ca^{2+} was entering mitochondria simply by a chemical gradient. Our results depicted on **Figure 7** support the latter assumption, since isolated mitochondria loaded with Fura-2 showed robust fluorescence-increases when perfused with high-Ca^{2+}, that

was only partially sensitive to Ru360 or RuRed. Thus we concluded that Ca^{2+} was acting indeed on an intramitochondrial site.

The presence of an uncoupler did not offer extra protection against Ca^{2+}-induced swelling and the uncoupler reversed the protective effect of substrates on WT mitochondria (**Figure 6 C, D, E** and **F**). Moreover, Complex I inhibition by rotenone and piericidin A granted protection against mitochondrial swelling provoked by Ca^{2+} even in the absence of substrates, that was not reproducible by blocking Complex I on a different site by high concentrations of the Complex III inhibitors myxothiazol and stigmatellin. On the other hand, inhibition of Complex III and IV rendered mitochondria supplied with substrates susceptible to swelling induced by Ca^{2+} (**Figure 8 A**, **B**, **C** and **Table 2**).

Complex IV inhibition of *in situ* mitochondria by KCN (equivalent of the substrate-starved state of isolated mitochondria) caused almost immediate swelling in both astrocytes and neurons irrespectively of functional or deleted CypD. However, the ablation of CypD had converse effect on depolarized *in situ* mitochondria in astrocytes and neurons, when the elapsed time before swelling due to Ca^{2+} overload was tested (**Figure 9 A** and **B**). Depolarized neuronal mitochondria with functional CypD were more resistant to Ca^{2+} overload, while depolarized mitochondria from astrocytes were protected by the ablation of CypD. On the other hand, *in situ*, non-depolarized and substrate-supplied neuronal mitochondria appear to be protected against Ca^{2+} overload (administration of a Ca^{2+} ionophore) and excitotoxicity (co-application of glutamate and glycine) by the ablation of CypD (**Figure 9 A**, first two columns, and **Figure 10**).

In **Section 4.2** attention was given to the NAADP-induced Ca^{2+}-release from hepatocyte mitochondria actively loaded by Ca^{2+} via SERCA and not V-type ATPases (**Figure 11 A**), which was comparable in magnitude to that mediated by $InsP_3$ and cADPR (**Figure 11 B** and **C**). Also, no cross-desensitization was present between the three pathways (**Figure 11 C**). NAADP released Ca^{2+} from hepatocyte microsomes in a

saturable manner with an EC_{50} of 0.93 ± 0.1 µM and maximal effect was recorded at concentrations higher than 2 µM (**Figure 12**). The special U-type self-desensitization curve of the NAADP-mediated Ca^{2+} release, that is a characteristic feature of NAADP, was detected in hepatocyte microsomes (**Figure 13**), as well as the relative pCa and pH independency of the Ca^{2+} efflux triggered by NAADP (**Figure 15 A** and **B**). By the use of thapsigargin and bafilomycin A, we demonstrated that the one-pool model for Ca^{2+} release is valid in the case of hepatocyte microsomes (**Figure 14**). The NAADP induced Ca^{2+} release was inhibited by verapamil and diltiazem while $InsP_3$ antagonists (e.g. heparin) and RyR inhibitors (ryanodine and RuRed) had no effect (**Figure 16** and **Table 3**).

Altogether, these data support the notion, that the NAADP-sensitive pathway for Ca^{2+} release from hepatocyte microsomes is indeed distinct from those triggered by $InsP_3$ and cADPR.

6. Summary

Cyclophilin-D (CypD) is a calcium-sensitive regulator of the permeability transition pore (PTP). In the present thesis, we show that substrate-deprived mitochondria obtained from CypD knock-out (KO) mice exhibit similar sensitivity to Ca^{2+}-induced PTP as wild type (WT) mitochondria exposed to cyclosporin-A. Our findings support the notion that the lack of an electrochemical gradient unfavoring electrophoretic Ca^{2+} uptake not only fails to protect in situ mitochondria from PTP, but it also subserves the purpose of decreasing a threshold to the point that induces pore opening. A further finding of this study is the dramatic hastening of the swelling of in situ neuronal and astrocytic mitochondria by glucose deprivation and NaCN co-application, upon calcimycin exposure. Our results also show that there are cell-specific differences of the same tissue regarding the contribution of CypD and the bioenergetic state to Ca^{2+}-induced PTP.

Nicotinic acid-adenine dinucleotide phosphate (NAADP) is rapidly emerging as an intracellular second messenger mediating Ca^{2+} release mainly from the acidic calcium stores, such as lysosomes and microsomes. In the present work, we demonstrate that the NAADP-mediated Ca^{2+}-release is indeed present in microsomes derived from rat hepatocytes and is relatively independent from changes of extravesicular Ca^{2+} concentrations and pH. For the first time in mammalian tissues, we provide evidence for the validity of the characteristic U-type self-desensitization curve of the NAADP-induced Ca^{2+}-release. Finally, we demonstrate that the NAADP-induced Ca^{2+} release is an independent Ca^{2+}-signalling pathway in rat hepatocyte microsomes based on its unique pharmacological-sensitivity profile and the lack of cross-desensitization between the $InsP_3$- cADPR- and NAADP-dependent Ca^{2+}-release systems.

7. Összefoglalás

A cyclophilin-D (CypD) a mitokondriális permeabilitás-tranzíciós pórus (PTP) calcium-függő szabályozó fehérjéje. Munkámban bemutatom, hogy CypD-génkiütött egerekből származó agyi mitokondriumok szubsztráthiányos körülmények között hasonló érzékenységet mutatnak a Ca^{2+}-indukált PT-vel szemben, mint a cyclosporin-A-val (CysA) kezelt vad típusú mitokondriumok. Eredményeim alátámasztják azt az elképzelést, mely szerint az elektrokémiai grádiens hiányában ellehetetlenülő elektroforetikus Ca^{2+} felvétel nem jelent védelmet az *in situ* mitokondriumban a PT-vel szemben, hanem ellenkezőleg, hozzájárul a pórus megnyílásához szükséges küszöb legyőzéséhez. Továbbá bemutatom, hogy a glükóz megvonása és NaCN együttes adása mellett az *in situ* neuronális és astrocyta mitokondriumok duzzadása drámai módon felgyorsul calcimycin alkalmazásakor. Eredményeim alapján elmondható, hogy a bioenergetikai állapota a sejtnek és a CypD adott szöveten belül sejt-specifikus módon járul hozzá a Ca^{2+}-indukált PT kiváltásához.

A nikotinsav-adenin dinukleotid foszfát (NAADP) egy olyan új intracellularis másodlagos hírvivő molekula, mely főként a savas Ca^{2+} raktárakból (pl. lizoszómákból és mikroszómákból) történő Ca^{2+} felszabadulásban vesz részt. Munkám során bemutatom, hogy az NAADP-indukált Ca^{2+}-kiáramlás patkány hepatocyta mikroszómákban is jelen van, valamint relatíve független a medium Ca^{2+}-koncentrációjától és pH-jától. Elsőként igazoltam az NAADP-mediált Ca^{2+}-felszabadulást alacsonyabb rendű szövetekben jellemző, U-típusú homológ deszenzitizáció érvényességét egy emlős szövetben. Az NAADP-indukált folyamat jellegzetes farmakológiai tulajdonságaira, illetve az NAADP-nek IP_3-mal és cADPR-zal mutatott kereszt-deszenzitizáció hiányára alapozva igazolom, hogy az NAADP-mediált Ca^{2+}-kiáramlás egy független és önálló Ca^{2+}-jelátviteli útvonal máj mikroszómákban.

List of publications

Related to the present thesis

1. Mándi M., Tóth B., Timár Gy. and Bak J. (2006): Ca^{2+} release triggered by NAADP in hepatocyte microsomes.
   Biochem. J. **395**: 233-238.
   [IF: 4.100]

2. Mándi M. & Bak J. (2008): Nicotinic acid adenine nucleotide dipohosphate (NAADP) and Ca^{2+} mobilization.
   J. Recept. Signal. Transduct. Res. **23 (3)**, 163-184.
   [IF: 1.540]

3. Chinopoulos, C., Vajda, S., Csanády, L., Mándi, M., Máthé, K., and Ádám-Vizi, V. (2009): A novel kinetic assay of mitochondrial ATP-ADP exchange rate mediated by the ANT.
   Biophys.J. **96**, 2490-2504.
   [IF: 4.390]

4. Vajda, S., Mándi, M., Konrád, C., Kiss, G., Ambrus, A., Ádám-Vizi, V., and Chinopoulos, C. (2009): A re-evaluation of the role of matrix acidification in uncoupler-induced Ca^{2+} release from mitochondria. FEBS J. **276**, 2713-2724.
   [IF: 3.042]

5. Chinopoulos, C., Gerencsér, AA., Mándi, M., Máthé, K., Törőcsik, B., Dóczi, J., Turiák, L., Kiss, G., Konrád, Cs., Vajda, Sz., Vereczki, V., Oh, RJ. and Ádám-Vizi, V. (2010): Forward operation of adenine nucleotide translocase during F0F1-ATPase reversal: critical role of matrix substrate-level phosphorylation. FASEB J. **24 (7)**, 2405-2416.
[IF: 6.401]

6. Dóczi, J., Turiák, L., Vajda Sz., Mándi, M., Törőcsik, B., Gerencsér, A.A., Kiss, G., Konrád, Cs., Ádám-Vizi, V., and Chinopoulos, C. (2011): Complex contribution of Cyclophilin-D to Ca^{2+}-induced permeability transition in brain mitochondria, with relation to the bioenergetic state.
J. Biol. Chem. **286 (8)**, 6345-6353.
[IF: 5.328]

Not related to the present thesis

7. Konrád, Cs.; Kiss, G.; Törőcsik, B.; Lábár, J.; Gerencsér, A.A.; Mándi, M.; Ádám-Vizi, V., and Chinopoulos, C. (2011): A distinct sequence in the adenine nucleotide translocase from Artemia franciscana embryos is associated with insensitivity to bongkrekate and atypical effects of adenine nucleotides on Ca^{2+} uptake and sequestration. FEBS J. **278 (5)**, 822-836.
[IF: 3.042]

Reference list

1 Berridge, M. J. Unlocking the secrets of cell signaling (2005) Annu.Rev.Physiol **67**, 1-21

2 Berridge, M. J., Bootman, M. D., and Roderick, H. L. Calcium signalling: dynamics, homeostasis and remodelling (2003) Nat.Rev.Mol.Cell Biol. **4**, 517-529

3 Clapham, D. E. TRP channels as cellular sensors (2003) Nature **426**, 517-524

4 Parekh, A. B. and Putney, J. W., Jr. Store-operated calcium channels (2005) Physiol Rev. **85**, 757-810

5 Verkhratsky, A. Physiology and pathophysiology of the calcium store in the endoplasmic reticulum of neurons (2005) Physiol Rev. **85**, 201-279

6 Rizzuto, R., Duchen, M. R., and Pozzan, T. Flirting in little space: the ER/mitochondria Ca^{2+} liaison (2004) Sci.STKE. **2004**, re1

7 Rudolf, R., Mongillo, M., Rizzuto, R., and Pozzan, T. Looking forward to seeing calcium (2003) Nat.Rev.Mol.Cell Biol. **4**, 579-586

8 Petersen, O. H. Calcium signal compartmentalization (2002) Biol.Res. **35**, 177-182

9 Pozzan, T., Rizzuto, R., Volpe, P., and Meldolesi, J. Molecular and cellular physiology of intracellular calcium stores (1994) Physiol Rev. **74**, 595-636

10 Streb, H., Irvine, R. F., Berridge, M. J., and Schulz, I. Release of Ca^{2+} from a nonmitochondrial intracellular store in pancreatic acinar cells by inositol-1,4,5-trisphosphate (1983) Nature **306**, 67-69

11 Eisen, A. and Reynolds, G. T. Source and sinks for the calcium released during fertilization of single sea urchin eggs (1985) J.Cell Biol. **100**, 1522-1527

12 Ganitkevich, V. Y. The role of mitochondria in cytoplasmic Ca^{2+} cycling (2003) Exp.Physiol **88**, 91-97

13 Hajnoczky, G., Robb-Gaspers, L. D., Seitz, M. B., and Thomas, A. P. Decoding of cytosolic calcium oscillations in the mitochondria (1995) Cell **82**, 415-424

14 Rizzuto, R., Brini, M., Murgia, M., and Pozzan, T. Microdomains with high Ca^{2+} close to IP_3-sensitive channels that are sensed by neighboring mitochondria (1993) Science **262**, 744-747

15 Pozzan, T. and Rizzuto, R. The renaissance of mitochondrial calcium transport (2000) Eur.J.Biochem. **267**, 5269-5273

16 Hansford, R. G. and Zorov, D. Role of mitochondrial calcium transport in the control of substrate oxidation (1998) Mol.Cell Biochem. **184**, 359-369

17 McCormack, J. G., Halestrap, A. P., and Denton, R. M. Role of calcium ions in regulation of mammalian intramitochondrial metabolism (1990) Physiol Rev. **70**, 391-425

18 Gunter, T. E. and Gunter, K. K. Uptake of calcium by mitochondria: transport and possible function (2001) IUBMB.Life **52**, 197-204

19 Reed, K. C. and Bygrave, F. L. A low molecular weight ruthenium complex inhibitory to mitochondrial Ca^{2+} transport (1974) FEBS Lett. **46**, 109-114

20 Moore, C. L. Specific inhibition of mitochondrial Ca^{2+} transport by ruthenium red (1971) Biochem.Biophys.Res.Commun. **42**, 298-305

21 Matlib, M. A., Zhou, Z., Knight, S., Ahmed, S., Choi, K. M., Krause-Bauer, J., Phillips, R., Altschuld, R., Katsube, Y., Sperelakis, N., and Bers, D. M. Oxygen-bridged dinuclear ruthenium amine complex specifically inhibits Ca^{2+} uptake into mitochondria in vitro and in situ in single cardiac myocytes (1998) J.Biol.Chem. **273**, 10223-10231

22 Bernardi, P., Paradisi, V., Pozzan, T., and Azzone, G. F. Pathway for uncoupler-induced calcium efflux in rat liver mitochondria: inhibition by ruthenium red (1984) Biochemistry **23**, 1645-1651

23 Bernardi, P. Mitochondrial transport of cations: channels, exchangers, and permeability transition (1999) Physiol Rev. **79**, 1127-1155

24 Pozzan, T., Magalhaes, P., and Rizzuto, R. The comeback of mitochondria to calcium signalling (2000) Cell Calcium **28**, 279-283

25 Sedova, M. and Blatter, L. A. Intracellular sodium modulates mitochondrial calcium signaling in vascular endothelial cells (2000) J.Biol.Chem. **275**, 35402-35407

26 Csordas, G. and Hajnoczky, G. Plasticity of mitochondrial calcium signaling (2003) J.Biol.Chem. **278**, 42273-42282

27 Moreau, B., Nelson, C., and Parekh, A. B. Biphasic regulation of mitochondrial Ca^{2+} uptake by cytosolic Ca^{2+} concentration (2006) Curr.Biol. **16**, 1672-1677

28 Giacomello, M., Drago, I., Pizzo, P., and Pozzan, T. Mitochondrial Ca^{2+} as a key regulator of cell life and death (2007) Cell Death. Differ. **14**, 1267-1274

29 Davidson, S. M. and Duchen, M. R. Calcium microdomains and oxidative stress (2006) Cell Calcium **40**, 561-574

30 Park, M. K., Ashby, M. C., Erdemli, G., Petersen, O. H., and Tepikin, A. V. Perinuclear, perigranular and sub-plasmalemmal mitochondria have distinct functions in the regulation of cellular calcium transport (2001) EMBO J. **20**, 1863-1874

31 Rizzuto, R. and Pozzan, T. Microdomains of intracellular Ca^{2+}: molecular determinants and functional consequences (2006) Physiol Rev. **86**, 369-408

32 Sparagna, G. C., Gunter, K. K., Sheu, S. S., and Gunter, T. E. Mitochondrial calcium uptake from physiological-type pulses of calcium. A description of the rapid uptake mode (1995) J.Biol.Chem. **270**, 27510-27515

33 Kirichok, Y., Krapivinsky, G., and Clapham, D. E. The mitochondrial calcium uniporter is a highly selective ion channel (2004) Nature **427**, 360-364

34 Gunter, T. E., Buntinas, L., Sparagna, G., Eliseev, R., and Gunter, K. Mitochondrial calcium transport: mechanisms and functions (2000) Cell Calcium **28**, 285-296

35 Bianchi, K., Rimessi, A., Prandini, A., Szabadkai, G., and Rizzuto, R. Calcium and mitochondria: mechanisms and functions of a troubled relationship (2004) Biochim.Biophys.Acta **1742**, 119-131

36 Altschafl, B. A., Beutner, G., Sharma, V. K., Sheu, S. S., and Valdivia, H. H. The mitochondrial ryanodine receptor in rat heart: a pharmaco-kinetic profile (2007) Biochim.Biophys.Acta **1768**, 1784-1795

37 Beutner, G., Sharma, V. K., Giovannucci, D. R., Yule, D. I., and Sheu, S. S. Identification of a ryanodine receptor in rat heart mitochondria (2001) J.Biol.Chem. **276**, 21482-21488

38 Beutner, G., Sharma, V. K., Lin, L., Ryu, S. Y., Dirksen, R. T., and Sheu, S. S. Type 1 ryanodine receptor in cardiac mitochondria: transducer of excitation-metabolism coupling (2005) Biochim.Biophys.Acta **1717**, 1-10

39 Pfeiffer, D. R., Gunter, T. E., Eliseev, R., Broekemeier, K. M., and Gunter, K. K. Release of Ca^{2+} from mitochondria via the saturable mechanisms and the permeability transition (2001) IUBMB.Life **52**, 205-212

40 Kaftan, E. J., Xu, T., Abercrombie, R. F., and Hille, B. Mitochondria shape hormonally induced cytoplasmic calcium

oscillations and modulate exocytosis (2000) J.Biol.Chem. **275**, 25465-25470

41 Chinopoulos, C., Starkov, A. A., Grigoriev, S., Dejean, L. M., Kinnally, K. W., Liu, X., Ambudkar, I. S., and Fiskum, G. Diacylglycerols activate mitochondrial cationic channel(s) and release sequestered $Ca^{(2+)}$ (2005) J.Bioenerg.Biomembr. **37**, 237-247

42 Bernardi, P., Krauskopf, A., Basso, E., Petronilli, V., Blachly-Dyson, E., Di Lisa, F., and Forte, M. A. The mitochondrial permeability transition from in vitro artifact to disease target (2006) FEBS J. **273**, 2077-2099

43 Ferri, K. F. and Kroemer, G. Organelle-specific initiation of cell death pathways (2001) Nat.Cell Biol. **3**, E255-E263

44 Ichas, F., Jouaville, L. S., and Mazat, J. P. Mitochondria are excitable organelles capable of generating and conveying electrical and calcium signals (1997) Cell **89**, 1145-1153

45 Chalmers, S. and Nicholls, D. G. The relationship between free and total calcium concentrations in the matrix of liver and brain mitochondria (2003) J.Biol.Chem. **278**, 19062-19070

46 Lehninger, A. L., Carafoli, E., and Rossi, C. S. Energy-linked ion movements in mitochondrial systems (1967) Adv.Enzymol.Relat Areas Mol.Biol. **29**, 259-320

47 Nicholls, D. G. Calcium transport and porton electrochemical potential gradient in mitochondria from guinea-pig cerebral cortex and rat heart (1978) Biochem.J. **170**, 511-522

48 Nicholls, D. G. and Chalmers, S. The integration of mitochondrial calcium transport and storage (2004) J.Bioenerg.Biomembr. **36**, 277-281

49 Chalmers, S. and Nicholls, D. G. The relationship between free and total calcium concentrations in the matrix of liver and brain mitochondria (2003) J.Biol.Chem. **278**, 19062-19070

50 Kristian, T., Pivovarova, N. B., Fiskum, G., and Andrews, S. B. Calcium-induced precipitate formation in brain mitochondria: composition, calcium capacity, and retention (2007) J.Neurochem. **102**, 1346-1356

51 Vajda, S., Mandi, M., Konrad, C., Kiss, G., Ambrus, A., Adam-Vizi, V., and Chinopoulos, C. A re-evaluation of the role of matrix acidification in uncoupler-induced Ca^{2+} release from mitochondria (2009) FEBS J. **276**, 2713-2724

52 Klingenberg, M. and Rottenberg, H. Relation between the gradient of the ATP/ADP ratio and the membrane potential across the mitochondrial membrane (1977) Eur.J.Biochem. **73**, 125-130

53 Chinopoulos, C., Vajda, S., Csanady, L., Mandi, M., Mathe, K., and Adam-Vizi, V. A novel kinetic assay of mitochondrial ATP-ADP exchange rate mediated by the ANT (2009) Biophys.J. **96**, 2490-2504

54 Nicholls, D. G. and Budd, S. L. Mitochondria and neuronal survival (2000) Physiol Rev. **80**, 315-360

55 Crompton, M. The mitochondrial permeability transition pore and its role in cell death (1999) Biochem.J. **341 (Pt 2)**, 233-249

56 Halestrap, A. P., Clarke, S. J., and Javadov, S. A. Mitochondrial permeability transition pore opening during myocardial reperfusion - a target for cardioprotection (2004) Cardiovasc.Res. **61**, 372-385

57 O'Reilly, C. M., Fogarty, K. E., Drummond, R. M., Tuft, R. A., and Walsh, J. V., Jr. Quantitative analysis of spontaneous mitochondrial depolarizations (2003) Biophys.J. **85**, 3350-3357

58 Vinogradov, A., Scarpa, A., and Chance, B. Calcium and pyridine nucleotide interaction in mitochondrial membranes (1972) Arch.Biochem.Biophys. **152**, 646-654

59 Bernardi, P. and Petronilli, V. The permeability transition pore as a mitochondrial calcium release channel: a critical appraisal (1996) J.Bioenerg.Biomembr. **28**, 131-138

60 Vergun, O., Votyakova, T. V., and Reynolds, I. J. Spontaneous changes in mitochondrial membrane potential in single isolated brain mitochondria (2003) Biophys.J. **85**, 3358-3366

61 Baines, C. P. The molecular composition of the mitochondrial permeability transition pore (2009) J.Mol.Cell Cardiol. **46**, 850-857

62 Crompton, M., Virji, S., Doyle, V., Johnson, N., and Ward, J. M. The mitochondrial permeability transition pore (1999) Biochem.Soc.Symp. **66**, 167-179

63 Klingenberg, M. and Nelson, D. R. Structure-function relationships of the ADP/ATP carrier (1994) Biochim.Biophys. Acta **1187**, 241-244

64 Pfaff, E., Klingenberg, M., and Heldt, H. W. Unspecific permeation and specific exchange of adenine nucleotides in liver mitochondria (1965) Biochim.Biophys.Acta **104**, 312-315

65 Pfaff, E., Heldt, H. W., and Klingenberg, M. Adenine nucleotide translocation of mitochondria. Kinetics of the adenine nucleotide exchange (1969) Eur.J.Biochem. **10**, 484-493

66 Beyer, K. and Klingenberg, M. ADP/ATP carrier protein from beef heart mitochondria has high amounts of tightly bound cardiolipin, as revealed by 31P nuclear magnetic resonance (1985) Biochemistry **24**, 3821-3826

67 Kokoszka, J. E., Waymire, K. G., Levy, S. E., Sligh, J. E., Cai, J., Jones, D. P., MacGregor, G. R., and Wallace, D. C. The ADP/ATP translocator is not essential for the mitochondrial permeability transition pore (2004) Nature **427**, 461-465

68 Baines, C. P., Kaiser, R. A., Sheiko, T., Craigen, W. J., and Molkentin, J. D. Voltage-dependent anion channels are dispensable for mitochondrial-dependent cell death (2007) Nat.Cell Biol. **9**, 550-555

69 Vyssokikh, M. Y. and Brdiczka, D. The function of complexes between the outer mitochondrial membrane pore (VDAC) and the adenine nucleotide translocase in regulation of energy metabolism and apoptosis (2003) Acta Biochim.Pol. **50**, 389-404

70 Brustovetsky, N. and Klingenberg, M. Mitochondrial ADP/ATP carrier can be reversibly converted into a large channel by Ca^{2+} (1996) Biochemistry **35**, 8483-8488

71 Clarke, S. J., McStay, G. P., and Halestrap, A. P. Sanglifehrin A acts as a potent inhibitor of the mitochondrial permeability transition and reperfusion injury of the heart by binding to cyclophilin-D at a different site from cyclosporin A (2002) J.Biol.Chem. **277**, 34793-34799

72 Scorrano, L., Nicolli, A., Basso, E., Petronilli, V., and Bernardi, P. Two modes of activation of the permeability transition pore: the role of mitochondrial cyclophilin (1997) Mol.Cell Biochem. **174**, 181-184

73 Hunter, D. R. and Haworth, R. A. The Ca^{2+}-induced membrane transition in mitochondria. I. The protective mechanisms (1979) Arch.Biochem.Biophys. **195**, 453-459

74 Halestrap, A. P. Calcium-dependent opening of a non-specific pore in the mitochondrial inner membrane is inhibited at pH values below 7. Implications for the protective effect of low pH against chemical and hypoxic cell damage (1991) Biochem.J. **278 (Pt 3)**, 715-719

75 Bernardi, P., Vassanelli, S., Veronese, P., Colonna, R., Szabo, I., and Zoratti, M. Modulation of the mitochondrial permeability transition pore. Effect of protons and divalent cations (1992) J.Biol.Chem. **267**, 2934-2939

76 McStay, G. P., Clarke, S. J., and Halestrap, A. P. Role of critical thiol groups on the matrix surface of the adenine nucleotide translocase in the mechanism of the mitochondrial permeability transition pore (2002) Biochem.J. **367**, 541-548

77 Halestrap, A. P., Kerr, P. M., Javadov, S., and Woodfield, K. Y. Elucidating the molecular mechanism of the permeability

transition pore and its role in reperfusion injury of the heart (1998) Biochim.Biophys.Acta **1366**, 79-94

78 Scorrano, L., Penzo, D., Petronilli, V., Pagano, F., and Bernardi, P. Arachidonic acid causes cell death through the mitochondrial permeability transition. Implications for tumor necrosis factor-alpha aopototic signaling (2001) J.Biol.Chem. **276**, 12035-12040

79 Bernardi, P., Veronese, P., and Petronilli, V. Modulation of the mitochondrial cyclosporin A-sensitive permeability transition pore. I. Evidence for two separate Me^{2+} binding sites with opposing effects on the pore open probability (1993) J.Biol.Chem. **268**, 1005-1010

80 Costantini, P., Chernyak, B. V., Petronilli, V., and Bernardi, P. Modulation of the mitochondrial permeability transition pore by pyridine nucleotides and dithiol oxidation at two separate sites (1996) J.Biol.Chem. **271**, 6746-6751

81 Bernardi, P. Modulation of the mitochondrial cyclosporin A-sensitive permeability transition pore by the proton electrochemical gradient. Evidence that the pore can be opened by membrane depolarization (1992) J.Biol.Chem. **267**, 8834-8839

82 Bernardi, P. Mitochondrial transport of cations: channels, exchangers, and permeability transition (1999) Physiol Rev. **79**, 1127-1155

83 Connern, C. P. and Halestrap, A. P. Purification and N-terminal sequencing of peptidyl-prolyl cis-trans-isomerase from rat liver mitochondrial matrix reveals the existence of a distinct mitochondrial cyclophilin (1992) Biochem.J. **284 (Pt 2)**, 381-385

84 Griffiths, E. J. and Halestrap, A. P. Further evidence that cyclosporin A protects mitochondria from calcium overload by inhibiting a matrix peptidyl-prolyl cis-trans isomerase. Implications for the immunosuppressive and toxic effects of cyclosporin (1991) Biochem.J. **274 (Pt 2)**, 611-614

85 Hausenloy, D. J., Duchen, M. R., and Yellon, D. M. Inhibiting mitochondrial permeability transition pore opening at reperfusion protects against ischaemia-reperfusion injury (2003) Cardiovasc.Res. **60**, 617-625

86 Reutenauer, J., Dorchies, O. M., Patthey-Vuadens, O., Vuagniaux, G., and Ruegg, U. T. Investigation of Debio 025, a cyclophilin inhibitor, in the dystrophic mdx mouse, a model for Duchenne muscular dystrophy (2008) Br.J.Pharmacol. **155**, 574-584

87 Nakagawa, T., Shimizu, S., Watanabe, T., Yamaguchi, O., Otsu, K., Yamagata, H., Inohara, H., Kubo, T., and Tsujimoto, Y. Cyclophilin D-dependent mitochondrial permeability transition regulates some necrotic but not apoptotic cell death (2005) Nature **434**, 652-658

88 Schinzel, A. C., Takeuchi, O., Huang, Z., Fisher, J. K., Zhou, Z., Rubens, J., Hetz, C., Danial, N. N., Moskowitz, M. A., and Korsmeyer, S. J. Cyclophilin D is a component of mitochondrial permeability transition and mediates neuronal cell death after focal cerebral ischemia (2005) Proc.Natl.Acad.Sci.U.S.A **102**, 12005-12010

89 Basso, E., Fante, L., Fowlkes, J., Petronilli, V., Forte, M. A., and Bernardi, P. Properties of the permeability transition pore in mitochondria devoid of Cyclophilin D (2005) J.Biol.Chem. **280**, 18558-18561

90 Baines, C. P., Kaiser, R. A., Purcell, N. H., Blair, N. S., Osinska, H., Hambleton, M. A., Brunskill, E. W., Sayen, M. R., Gottlieb, R. A., Dorn, G. W., Robbins, J., and Molkentin, J. D. Loss of cyclophilin D reveals a critical role for mitochondrial permeability transition in cell death (2005) Nature **434**, 658-662

91 Luvisetto, S., Basso, E., Petronilli, V., Bernardi, P., and Forte, M. Enhancement of anxiety, facilitation of avoidance behavior, and occurrence of adult-onset obesity in mice lacking mitochondrial cyclophilin D (2008) Neuroscience **155**, 585-596

92 Jobe, S. M., Wilson, K. M., Leo, L., Raimondi, A., Molkentin, J. D., Lentz, S. R., and Di Paola, J. Critical role for the mitochondrial permeability transition pore and cyclophilin D in platelet activation and thrombosis (2008) Blood **111**, 1257-1265

93 Baines, C. P., Kaiser, R. A., Purcell, N. H., Blair, N. S., Osinska, H., Hambleton, M. A., Brunskill, E. W., Sayen, M. R., Gottlieb, R. A., Dorn, G. W., Robbins, J., and Molkentin, J. D. Loss of cyclophilin D reveals a critical role for mitochondrial permeability transition in cell death (2005) Nature **434**, 658-662

94 Du, H., Guo, L., Fang, F., Chen, D., Sosunov, A. A., McKhann, G. M., Yan, Y., Wang, C., Zhang, H., Molkentin, J. D., Gunn-Moore, F. J., Vonsattel, J. P., Arancio, O., Chen, J. X., and Yan, S. D. Cyclophilin D deficiency attenuates mitochondrial and neuronal perturbation and ameliorates learning and memory in Alzheimer's disease (2008) Nat.Med. **14**, 1097-1105

95 Elrod, J. W., Wong, R., Mishra, S., Vagnozzi, R. J., Sakthievel, B., Goonasekera, S. A., Karch, J., Gabel, S., Farber, J., Force, T., Brown, J. H., Murphy, E., and Molkentin, J. D. Cyclophilin D controls mitochondrial pore-dependent Ca($^{2+}$) exchange, metabolic

flexibility, and propensity for heart failure in mice (2010) J.Clin.Invest **120**, 3680-3687

96 Millay, D. P., Sargent, M. A., Osinska, H., Baines, C. P., Barton, E. R., Vuagniaux, G., Sweeney, H. L., Robbins, J., and Molkentin, J. D. Genetic and pharmacologic inhibition of mitochondrial-dependent necrosis attenuates muscular dystrophy (2008) Nat.Med. **14**, 442-447

97 Halestrap, A. P. What is the mitochondrial permeability transition pore? (2009) J.Mol.Cell Cardiol. **46**, 821-831

98 Giorgio, V., Bisetto, E., Soriano, M. E., Dabbeni-Sala, F., Basso, E., Petronilli, V., Forte, M. A., Bernardi, P., and Lippe, G. Cyclophilin D modulates mitochondrial F0F1-ATP synthase by interacting with the lateral stalk of the complex (2009) J.Biol.Chem. **284**, 33982-33988

99 Basso, E., Petronilli, V., Forte, M. A., and Bernardi, P. Phosphate is essential for inhibition of the mitochondrial permeability transition pore by cyclosporin A and by cyclophilin D ablation (2008) J.Biol.Chem. **283**, 26307-26311

100 Chinopoulos, C. and Adam-Vizi, V. Modulation of The Mitochondrial Permeability Transition by Cyclophilin D: One Step Closer Towards F_oF_1 ATP synthase? Manuscript . 2010.

101 Li, Y., Johnson, N., Capano, M., Edwards, M., and Crompton, M. Cyclophilin-D promotes the mitochondrial permeability transition but has opposite effects on apoptosis and necrosis (2004) Biochem.J. **383**, 101-109

102 Doczi, J., Turiak, L., Vajda, S., Mandi, M., Torocsik, B., Gerencser, A. A., Kiss, G., Konrad, C., Adam-Vizi, V., and Chinopoulos, C. Complex contribution of cyclophilin D to Ca^{2+}-induced permeability transition in brain mitochondria, with relation to the bioenergetic state (2010) J.Biol.Chem.

103 Clapper, D. L., Walseth, T. F., Dargie, P. J., and Lee, H. C. Pyridine nucleotide metabolites stimulate calcium release from sea urchin egg microsomes desensitized to inositol trisphosphate (1987) J.Biol.Chem. **262**, 9561-9568

104 Dousa, T. P., Chini, E. N., and Beers, K. W. Adenine nucleotide diphosphates: emerging second messengers acting via intracellular Ca^{2+} release (1996) Am.J.Physiol **271**, C1007-C1024

105 Galione, A., Patel, S., and Churchill, G. C. NAADP-induced calcium release in sea urchin eggs (2000) Biol.Cell **92**, 197-204

106 Lee, H. C. Mechanisms of calcium signaling by cyclic ADP-ribose and NAADP (1997) Physiol Rev. **77**, 1133-1164

107 Lee, H. C. Physiological functions of cyclic ADP-ribose and NAADP as calcium messengers (2001) Annu.Rev.Pharmacol. Toxicol. **41**, 317-345

108 Lee, H. C., Walseth, T. F., Bratt, G. T., Hayes, R. N., and Clapper, D. L. Structural determination of a cyclic metabolite of NAD^+ with intracellular Ca^{2+}-mobilizing activity (1989) J.Biol.Chem. **264**, 1608-1615

109 Lee, H. C. and Aarhus, R. A derivative of NADP mobilizes calcium stores insensitive to inositol trisphosphate and cyclic ADP-ribose (1995) J.Biol.Chem. **270**, 2152-2157

110 Cancela, J. M., Churchill, G. C., and Galione, A. Coordination of agonist-induced Ca^{2+}-signalling patterns by NAADP in pancreatic acinar cells (1999) Nature **398**, 74-76

111 Cancela, J. M., Charpentier, G., and Petersen, O. H. Co-ordination of Ca^{2+} signalling in mammalian cells by the new Ca^{2+}-releasing messenger NAADP (2003) Pflugers Arch. **446**, 322-327

112 Galione, A. and Petersen, O. H. The NAADP receptor: new receptors or new regulation? (2005) Mol.Interv. **5**, 73-79

113 Masgrau, R., Churchill, G. C., Morgan, A. J., Ashcroft, S. J., and Galione, A. NAADP: a new second messenger for glucose-induced Ca^{2+} responses in clonal pancreatic beta cells (2003) Curr.Biol. **13**, 247-251

114 Navazio, L., Bewell, M. A., Siddiqua, A., Dickinson, G. D., Galione, A., and Sanders, D. Calcium release from the endoplasmic reticulum of higher plants elicited by the NADP metabolite nicotinic acid adenine dinucleotide phosphate (2000) Proc.Natl.Acad.Sci.U.S.A **97**, 8693-8698

115 Patel, S., Churchill, G. C., and Galione, A. Coordination of Ca^{2+} signalling by NAADP (2001) Trends Biochem.Sci. **26**, 482-489

116 Mandi, M., Toth, B., Timar, G., and Bak, J. Ca^{2+} release triggered by NAADP in hepatocyte microsomes (2006) Biochem.J. **395**, 233-238

117 Bak, J., White, P., Timar, G., Missiaen, L., Genazzani, A. A., and Galione, A. Nicotinic acid adenine dinucleotide phosphate triggers Ca^{2+} release from brain microsomes (1999) Curr.Biol. **9**, 751-754

118 Bak, J., Billington, R. A., Timar, G., Dutton, A. C., and Genazzani, A. A. NAADP receptors are present and functional in the heart (2001) Curr.Biol. **11**, 987-990

119 Cheng, J., Yusufi, A. N., Thompson, M. A., Chini, E. N., and Grande, J. P. Nicotinic acid adenine dinucleotide phosphate: a new Ca^{2+} releasing agent in kidney (2001) J.Am.Soc.Nephrol. **12**, 54-60

120 Berg, I., Potter, B. V., Mayr, G. W., and Guse, A. H. Nicotinic acid adenine dinucleotide phosphate ($NAADP^{+}$) is an essential regulator of T-lymphocyte Ca^{2+}-signaling (2000) J.Cell Biol. **150**, 581-588

121 Hohenegger, M., Suko, J., Gscheidlinger, R., Drobny, H., and Zidar, A. Nicotinic acid-adenine dinucleotide phosphate activates the skeletal muscle ryanodine receptor (2002) Biochem.J. **367**, 423-431

122 Yusufi, A. N., Cheng, J., Thompson, M. A., Chini, E. N., and Grande, J. P. Nicotinic acid-adenine dinucleotide phosphate (NAADP) elicits specific microsomal Ca^{2+} release from mammalian cells (2001) Biochem.J. **353**, 531-536

123 Zhang, F. and Li, P. L. Reconstitution and characterization of a nicotinic acid adenine dinucleotide phosphate (NAADP)-sensitive Ca^{2+} release channel from liver lysosomes of rats (2007) J.Biol.Chem. **282**, 25259-25269

124 Chini, E. N., Chini, C. C., Kato, I., Takasawa, S., and Okamoto, H. CD38 is the major enzyme responsible for synthesis of nicotinic acid-adenine dinucleotide phosphate in mammalian tissues (2002) Biochem.J. **362**, 125-130

125 Berridge, G., Dickinson, G., Parrington, J., Galione, A., and Patel, S. Solubilization of receptors for the novel Ca^{2+}-mobilizing messenger, nicotinic acid adenine dinucleotide phosphate (2002) J.Biol.Chem. **277**, 43717-43723

126 Galione, A. and Ruas, M. NAADP receptors (2005) Cell Calcium **38**, 273-280

127 Aarhus, R., Dickey, D. M., Graeff, R. M., Gee, K. R., Walseth, T. F., and Lee, H. C. Activation and inactivation of Ca^{2+} release by $NAADP^{+}$ (1996) J.Biol.Chem. **271**, 8513-8516

128 Billington, R. A. and Genazzani, A. A. Characterization of $NAADP^{+}$ binding in sea urchin eggs (2000) Biochem.Biophys. Res.Commun. **276**, 112-116

129 Patel, S., Churchill, G. C., Sharp, T., and Galione, A. Widespread distribution of binding sites for the novel Ca^{2+}-mobilizing messenger, nicotinic acid adenine dinucleotide phosphate, in the brain (2000) J.Biol.Chem. **275**, 36495-36497

130 Genazzani, A. A., Empson, R. M., and Galione, A. Unique inactivation properties of NAADP-sensitive Ca^{2+} release (1996) J.Biol.Chem. **271**, 11599-11602

131 Bak, J., Billington, R. A., and Genazzani, A. A. Effect of luminal and extravesicular Ca^{2+} on NAADP binding and release properties (2002) Biochem.Biophys.Res.Commun. **295**, 806-811

132 Dammermann, W. and Guse, A. H. Functional ryanodine receptor expression is required for NAADP-mediated local Ca^{2+} signaling in T-lymphocytes (2005) J.Biol.Chem. **280**, 21394-21399

133 Langhorst, M. F., Schwarzmann, N., and Guse, A. H. Ca^{2+} release via ryanodine receptors and Ca^{2+} entry: major mechanisms in NAADP-mediated Ca^{2+} signaling in T-lymphocytes (2004) Cell Signal. **16**, 1283-1289

134 Gerasimenko, J. V., Maruyama, Y., Yano, K., Dolman, N. J., Tepikin, A. V., Petersen, O. H., and Gerasimenko, O. V. NAADP mobilizes Ca^{2+} from a thapsigargin-sensitive store in the nuclear envelope by activating ryanodine receptors (2003) J.Cell Biol. **163**, 271-282

135 Mojzisova, A., Krizanova, O., Zacikova, L., Kominkova, V., and Ondrias, K. Effect of nicotinic acid adenine dinucleotide phosphate on ryanodine calcium release channel in heart (2001) Pflugers Arch. **441**, 674-677

136 Bezin, S., Charpentier, G., Fossier, P., and Cancela, J. M. The Ca^{2+}-releasing messenger NAADP, a new player in the nervous system (2006) J.Physiol Paris **99**, 111-118

137 Zong, X., Schieder, M., Cuny, H., Fenske, S., Gruner, C., Rotzer, K., Griesbeck, O., Harz, H., Biel, M., and Wahl-Schott, C. The two-pore channel TPCN2 mediates NAADP-dependent $Ca(^{2+})$-release from lysosomal stores (2009) Pflugers Arch. **458**, 891-899

138 Calcraft, P. J., Ruas, M., Pan, Z., Cheng, X., Arredouani, A., Hao, X., Tang, J., Rietdorf, K., Teboul, L., Chuang, K. T., Lin, P., Xiao, R., Wang, C., Zhu, Y., Lin, Y., Wyatt, C. N., Parrington, J., Ma, J., Evans, A. M., Galione, A., and Zhu, M. X. NAADP mobilizes calcium from acidic organelles through two-pore channels (2009) Nature **459**, 596-600

139 Churchill, G. C., Okada, Y., Thomas, J. M., Genazzani, A. A., Patel, S., and Galione, A. NAADP mobilizes Ca($^{2+}$) from reserve granules, lysosome-related organelles, in sea urchin eggs (2002) Cell **111**, 703-708

140 Heidemann, A. C., Schipke, C. G., and Kettenmann, H. Extracellular application of nicotinic acid adenine dinucleotide phosphate induces Ca^{2+} signaling in astrocytes in situ (2005) J.Biol.Chem. **280**, 35630-35640

141 Yamasaki, M., Masgrau, R., Morgan, A. J., Churchill, G. C., Patel, S., Ashcroft, S. J., and Galione, A. Organelle selection determines agonist-specific Ca^{2+} signals in pancreatic acinar and beta cells (2004) J.Biol.Chem. **279**, 7234-7240

142 Yamasaki, M., Thomas, J. M., Churchill, G. C., Garnham, C., Lewis, A. M., Cancela, J. M., Patel, S., and Galione, A. Role of NAADP and cADPR in the induction and maintenance of agonist-evoked Ca^{2+} spiking in mouse pancreatic acinar cells (2005) Curr.Biol. **15**, 874-878

143 Mitchell, K. J., Lai, F. A., and Rutter, G. A. Ryanodine receptor type I and nicotinic acid adenine dinucleotide phosphate receptors mediate Ca^{2+} release from insulin-containing vesicles in living pancreatic beta-cells (MIN6) (2003) J.Biol.Chem. **278**, 11057-11064

144 Jadot, M., Andrianaivo, F., Dubois, F., and Wattiaux, R. Effects of methylcyclodextrin on lysosomes (2001) Eur.J.Biochem. **268**, 1392-1399

145 Morgan, A. J. and Galione, A. NAADP induces pH changes in the lumen of acidic Ca^{2+} stores (2007) Biochem.J. **402**, 301-310

146 Brailoiu, E., Hoard, J. L., Filipeanu, C. M., Brailoiu, G. C., Dun, S. L., Patel, S., and Dun, N. J. Nicotinic acid adenine dinucleotide phosphate potentiates neurite outgrowth (2005) J.Biol.Chem. **280**, 5646-5650

147 Kinnear, N. P., Boittin, F. X., Thomas, J. M., Galione, A., and Evans, A. M. Lysosome-sarcoplasmic reticulum junctions. A trigger zone for calcium signaling by nicotinic acid adenine dinucleotide phosphate and endothelin-1 (2004) J.Biol.Chem. **279**, 54319-54326

148 Lim, D., Kyozuka, K., Gragnaniello, G., Carafoli, E., and Santella, L. $NAADP^+$ initiates the Ca^{2+} response during fertilization of starfish oocytes (2001) FASEB J. **15**, 2257-2267

149 Cancela, J. M., Gerasimenko, O. V., Gerasimenko, J. V., Tepikin, A. V., and Petersen, O. H. Two different but converging messenger pathways to intracellular Ca^{2+} release: the roles of nicotinic acid adenine dinucleotide phosphate, cyclic ADP-ribose and inositol trisphosphate (2000) EMBO J. **19**, 2549-2557

150 Churchill, G. C. and Galione, A. NAADP induces Ca^{2+} oscillations via a two-pool mechanism by priming IP_3- and cADPR-sensitive Ca^{2+} stores (2001) EMBO J. **20**, 2666-2671

151 Churchill, G. C. and Galione, A. Spatial control of Ca^{2+} signaling by nicotinic acid adenine dinucleotide phosphate diffusion and gradients (2000) J.Biol.Chem. **275**, 38687-38692

152 Billington, R. A., Ho, A., and Genazzani, A. A. Nicotinic acid adenine dinucleotide phosphate (NAADP) is present at micromolar concentrations in sea urchin spermatozoa (2002) J.Physiol **544**, 107-112

153 Churamani, D., Carrey, E. A., Dickinson, G. D., and Patel, S. Determination of cellular nicotinic acid-adenine dinucleotide phosphate (NAADP) levels (2004) Biochem.J. **380**, 449-454

154 Churchill, G. C., O'Neill, J. S., Masgrau, R., Patel, S., Thomas, J. M., Genazzani, A. A., and Galione, A. Sperm deliver a new second messenger: NAADP (2003) Curr.Biol. **13**, 125-128

155 Wilson, H. L. and Galione, A. Differential regulation of nicotinic acid-adenine dinucleotide phosphate and cADP-ribose production by cAMP and cGMP (1998) Biochem.J. **331 (Pt 3)**, 837-843

156 Chini, E. N. and De Toledo, F. G. Nicotinic acid adenine dinucleotide phosphate: a new intracellular second messenger? (2002) Am.J.Physiol Cell Physiol **282**, C1191-C1198

157 Bruzzone, S., Guida, L., Zocchi, E., Franco, L., and De Flora, A. Connexin 43 hemi channels mediate Ca^{2+}-regulated transmembrane NAD+ fluxes in intact cells (2001) FASEB J. **15**, 10-12

158 Guida, L., Bruzzone, S., Sturla, L., Franco, L., Zocchi, E., and De Flora, A. Equilibrative and concentrative nucleoside transporters mediate influx of extracellular cyclic ADP-ribose into 3T3 murine fibroblasts (2002) J.Biol.Chem. **277**, 47097-47105

159 Billington, R. A., Bellomo, E. A., Floriddia, E. M., Erriquez, J., Distasi, C., and Genazzani, A. A. A transport mechanism for NAADP in a rat basophilic cell line (2006) FASEB J. **20**, 521-523

160 Liang, M., Chini, E. N., Cheng, J., and Dousa, T. P. Synthesis of NAADP and cADPR in mitochondria (1999) Arch.Biochem. Biophys. **371**, 317-325

161 Ceni, C., Muller-Steffner, H., Lund, F., Pochon, N., Schweitzer, A., De Waard, M., Schuber, F., Villaz, M., and Moutin, M. J. Evidence for an intracellular ADP-ribosyl cyclase/NAD^+-glycohydrolase in brain from CD38-deficient mice (2003) J.Biol.Chem. **278**, 40670-40678

162 Soares, S., Thompson, M., White, T., Isbell, A., Yamasaki, M., Prakash, Y., Lund, F. E., Galione, A., and Chini, E. N. NAADP as a second messenger: neither CD38 nor base-exchange reaction are necessary for in vivo generation of NAADP in myometrial cells (2007) Am.J.Physiol Cell Physiol **292**, C227-C239

163 Burdakov, D. and Galione, A. Two neuropeptides recruit different messenger pathways to evoke Ca^{2+} signals in the same cell (2000) Curr.Biol. **10**, 993-996

164 Cancela, J. M. Specific Ca^{2+} signaling evoked by cholecystokinin and acetylcholine: the roles of NAADP, cADPR, and IP_3 (2001) Annu.Rev.Physiol **63**, 99-117

165 Cancela, J. M., Van Coppenolle, F., Galione, A., Tepikin, A. V., and Petersen, O. H. Transformation of local Ca^{2+} spikes to global Ca^{2+} transients: the combinatorial roles of multiple Ca^{2+} releasing messengers (2002) EMBO J. **21**, 909-919

166 Gerasimenko, J. V., Flowerdew, S. E., Voronina, S. G., Sukhomlin, T. K., Tepikin, A. V., Petersen, O. H., and Gerasimenko, O. V. Bile acids induce Ca^{2+} release from both the endoplasmic reticulum and acidic intracellular calcium stores through activation of inositol trisphosphate receptors and ryanodine receptors (2006) J.Biol.Chem. **281**, 40154-40163

167 Chameau, P., Van, d., V, Fossier, P., and Baux, G. Ryanodine-, IP_3- and NAADP-dependent calcium stores control acetylcholine release (2001) Pflugers Arch. **443**, 289-296

168 Mandi, M. and Bak, J. Nicotinic acid adenine dinucleotide phosphate (NAADP) and Ca^{2+} mobilization (2008) J.Recept.Signal.Transduct.Res. **28**, 163-184

169 Sims, N. R. Rapid isolation of metabolically active mitochondria from rat brain and subregions using Percoll density gradient centrifugation (1990) J.Neurochem. **55**, 698-707

170 Chinopoulos, C., Starkov, A. A., and Fiskum, G. Cyclosporin A-insensitive permeability transition in brain mitochondria: inhibition by 2-aminoethoxydiphenyl borate (2003) J.Biol.Chem. **278**, 27382-27389

171 Fleschner, C. R. and Kraus-Friedmann, N. The effect of Mg^{2+} on hepatic microsomal Ca^{2+} and Sr^{2+} transport (1986) Eur.J.Biochem. **154**, 313-320

172 Akerman, K. E. and Wikstrom, M. K. Safranine as a probe of the mitochondrial membrane potential (1976) FEBS Lett. **68**, 191-197

173 Schonfeld, P. Does the function of adenine nucleotide translocase in fatty acid uncoupling depend on the type of mitochondria? (1990) FEBS Lett. **264**, 246-248

174 Nicolli, A., Petronilli, V., and Bernardi, P. Modulation of the mitochondrial cyclosporin A-sensitive permeability transition pore by matrix pH. Evidence that the pore open-closed probability is regulated by reversible histidine protonation (1993) Biochemistry **32**, 4461-4465

175 Selwyn, M. J., Dawson, A. P., and Dunnett, S. J. Calcium transport in mitochondria (1970) FEBS Lett. **10**, 1-5

176 Moore, G. A., Jewell, S. A., Bellomo, G., and Orrenius, S. On the relationship between Ca^{2+} efflux and membrane damage during t-butylhydroperoxide metabolism by liver mitochondria (1983) FEBS Lett. **153**, 289-292

177 Rigobello, M. P., Turcato, F., and Bindoli, A. Inhibition of rat liver mitochondrial permeability transition by respiratory substrates (1995) Arch.Biochem.Biophys. **319**, 225-230

178 Yamamoto, T., Yoshimura, Y., Yamada, A., Gouda, S., Yamashita, K., Yamazaki, N., Kataoka, M., Nagata, T., Terada, H., and Shinohara, Y. Distinct behaviors of adenylate kinase and cytochrome c observed following induction of mitochondrial permeability transition by Ca^{2+} in the absence of respiratory substrate (2008) J.Bioenerg.Biomembr. **40**, 619-623

179 Leverve, X. M. and Fontaine, E. Role of substrates in the regulation of mitochondrial function in situ (2001) IUBMB.Life **52**, 221-229

180 Brustovetsky, N. and Dubinsky, J. M. Limitations of cyclosporin A inhibition of the permeability transition in CNS mitochondria (2000) J.Neurosci. **20**, 8229-8237

181 Degli Esposti M. Inhibitors of NADH-ubiquinone reductase: an overview (1998) Biochim.Biophys.Acta **1364**, 222-235

182 Chauvin, C., De Oliveira, F., Ronot, X., Mousseau, M., Leverve, X., and Fontaine, E. Rotenone inhibits the mitochondrial

permeability transition-induced cell death in U937 and KB cells (2001) J.Biol.Chem. **276**, 41394-41398

183 Gerencser, A. A., Doczi, J., Torocsik, B., Bossy-Wetzel, E., and Adam-Vizi, V. Mitochondrial swelling measurement in situ by optimized spatial filtering: astrocyte-neuron differences (2008) Biophys.J. **95**, 2583-2598

184 Grynkiewicz, G., Poenie, M., and Tsien, R. Y. A new generation of Ca^{2+} indicators with greatly improved fluorescence properties (1985) J.Biol.Chem. **260**, 3440-3450

185 Chinopoulos, C., Gerencser, A. A., Doczi, J., Fiskum, G., and Adam-Vizi, V. Inhibition of glutamate-induced delayed calcium deregulation by 2-APB and La^{3+} in cultured cortical neurones (2004) J.Neurochem. **91**, 471-483

186 Nicholls, D. G. and Ward, M. W. Mitochondrial membrane potential and neuronal glutamate excitotoxicity: mortality and millivolts (2000) Trends Neurosci. **23**, 166-174

187 Sattler, R. and Tymianski, M. Molecular mechanisms of glutamate receptor-mediated excitotoxic neuronal cell death (2001) Mol.Neurobiol. **24**, 107-129

188 Petronilli, V., Cola, C., Massari, S., Colonna, R., and Bernardi, P. Physiological effectors modify voltage sensing by the cyclosporin A-sensitive permeability transition pore of mitochondria (1993) J.Biol.Chem. **268**, 21939-21945

189 Petronilli, V., Cola, C., and Bernardi, P. Modulation of the mitochondrial cyclosporin A-sensitive permeability transition pore. II. The minimal requirements for pore induction underscore a

key role for transmembrane electrical potential, matrix pH, and matrix Ca^{2+} (1993) J.Biol.Chem. **268**, 1011-1016

190 Petronilli, V., Costantini, P., Scorrano, L., Colonna, R., Passamonti, S., and Bernardi, P. The voltage sensor of the mitochondrial permeability transition pore is tuned by the oxidation-reduction state of vicinal thiols. Increase of the gating potential by oxidants and its reversal by reducing agents (1994) J.Biol.Chem. **269**, 16638-16642

191 Scorrano, L., Petronilli, V., and Bernardi, P. On the voltage dependence of the mitochondrial permeability transition pore. A critical appraisal (1997) J.Biol.Chem. **272**, 12295-12299

192 Fontaine, E., Eriksson, O., Ichas, F., and Bernardi, P. Regulation of the permeability transition pore in skeletal muscle mitochondria. Modulation By electron flow through the respiratory chain complex i (1998) J.Biol.Chem. **273**, 12662-12668

193 Ryan, M. T. and Hoogenraad, N. J. Mitochondrial-nuclear communications (2007) Annu.Rev.Biochem. **76**, 701-722

194 Panov, A., Dikalov, S., Shalbuyeva, N., Hemendinger, R., Greenamyre, J. T., and Rosenfeld, J. Species- and tissue-specific relationships between mitochondrial permeability transition and generation of ROS in brain and liver mitochondria of rats and mice (2007) Am.J.Physiol Cell Physiol **292**, C708-C718

195 Zorov, D. B., Juhaszova, M., Yaniv, Y., Nuss, H. B., Wang, S., and Sollott, S. J. Regulation and pharmacology of the mitochondrial permeability transition pore (2009) Cardiovasc.Res. **83**, 213-225

196 Lilly, L. B. and Gollan, J. L. Ryanodine-induced calcium release from hepatic microsomes and permeabilized hepatocytes (1995) Am.J.Physiol **268**, G1017-G1024

197 Bowman, E. J., Siebers, A., and Altendorf, K. Bafilomycins: a class of inhibitors of membrane ATPases from microorganisms, animal cells, and plant cells (1988) Proc.Natl.Acad.Sci.U.S.A **85**, 7972-7976

198 Genazzani, A. A. and Galione, A. Nicotinic acid-adenine dinucleotide phosphate mobilizes Ca^{2+} from a thapsigargin-insensitive pool (1996) Biochem.J. **315 (Pt 3)**, 721-725

199 Hagar, R. E., Burgstahler, A. D., Nathanson, M. H., and Ehrlich, B. E. Type III $InsP_3$ receptor channel stays open in the presence of increased calcium (1998) Nature **396**, 81-84

200 Meszaros, L. G., Bak, J., and Chu, A. Cyclic ADP-ribose as an endogenous regulator of the non-skeletal type ryanodine receptor Ca^{2+} channel (1993) Nature **364**, 76-79

201 Chini, E. N., Liang, M., and Dousa, T. P. Differential effect of pH upon cyclic-ADP-ribose and nicotinate-adenine dinucleotide phosphate-induced Ca^{2+} release systems (1998) Biochem.J. **335 (Pt 3)**, 499-504

202 Genazzani, A. A., Mezna, M., Dickey, D. M., Michelangeli, F., Walseth, T. F., and Galione, A. Pharmacological properties of the Ca^{2+}-release mechanism sensitive to NAADP in the sea urchin egg (1997) Br.J.Pharmacol. **121**, 1489-1495

203 Chinopoulos, C., Gerencser, A. A., Mandi, M., Mathe, K., Torocsik, B., Doczi, J., Turiak, L., Kiss, G., Konrad, C., Vajda, S., Vereczki, V., Oh, R. J., and Adam-Vizi, V. Forward operation of adenine nucleotide translocase during F_0F_1-ATPase reversal: critical role of matrix substrate-level phosphorylation (2010) FASEB J. **24 (7)**, 2405-2416

Acknowledgements

I would like to express my gratitude to my supervisor, Professor Veronika Ádám, who provided me the opportunity for carrying out experiments in the Department of Medical Biochemistry and provided a solid basis for the composition of the present PhD thesis.

I am very grateful to my tutor and supervisor, Dr. Christos Chinopoulos, who introduced me to the world of mitochondriology and fluorimetry with endless enthusiasm, energy, motivation and immense knowledge of this field. I wish to thank his for his patience, stimulating suggestions and objective criticism during the experiments.

I wish to thank Dr. Judit Bak all the help, guidance and support ever since the beginning of my scientific career. I will always be grateful for her, not only for teaching me the basis of experimenting with microsomes and isotopes, the planning of experimental procedures and the ins and outs of composing manuscripts, posters and lectures, but also for our friendship.

My special thanks go to all my collegues in the Department of Medical Biochemistry for their support, friendship and helpful discussions.

Finally, I would like to thank my loving wife, Barbara Mándi-Fehér for the „home” and solid background that she provides, without which I could never have accomplished any of my professional or scientific results. She is nursing our firstborn child, Levente Máté with endless love and caring. I wish to thank my mother and father, my brother, my cousin and my mother-in-law for their never fading support, love and faith.